IEEE Access
Multidisciplinary : Rapid Review : Open Access Journal

Received February 17, 2020, accepted February 28, 2020, date of publication March 10, 2020, date of current version April 8, 2020.

Digital Object Identifier 10.1109/ACCESS.2020.2979927

Improvements in the Explicit Estimation of Pollutant Dispersion Coefficient in Rivers by Subset Selection of Maximum Dissimilarity Hybridized With ANFIS-Firefly Algorithm (FFA)

HOSSIEN RIAHI-MADVAR[1], MAJID DEHGHANI[2], KULWINDER SINGH PARMAR[3], NARJES NABIPOUR[4], AND SHAHABODDIN SHAMSHIRBAND[5,6]

[1]Department of Water Science and Engineering, Faculty of Agriculture, Vali-e-Asr University of Rafsanjan, Rafsanjan 7718897111, Iran
[2]Department of Civil Engineering, Faculty of Technical and Engineering, Vali-e-Asr University of Rafsanjan, Rafsanjan 7718897111, Iran
[3]Department of Mathematics, I. K. Gujral Punjab Technical University, Jalandhar-Kapurthala 144603, India
[4]Institute of Research and Development, Duy Tan University, Da Nang 550000, Vietnam
[5]Department for Management of Science and Technology Development, Ton Duc Thang University, Ho Chi Minh City, Vietnam
[6]Faculty of Information Technology, Ton Duc Thang University, Ho Chi Minh City, Vietnam

Corresponding author: Shahaboddin Shamshirband (shahaboddin.shamshirband@tdtu.edu.vn)

ABSTRACT In this paper, a new hybrid model is proposed using Subset Selection by Maximum Dissimilarity (SSMD) and adaptive neuro-fuzzy inference system (ANFIS) hybridized with the firefly algorithm (FFA) to predict the longitudinal dispersion coefficient (K_x). The proposed framework (ANFIS-FFA), combines the specific structures and strengths of both ANFIS and FFA approaches. The FFA is used to derive the optimum ANFIS parameters. The K_x data set includes 503 cross-sectional data point from small to large rivers. For pre-processing of the data set, the SSMD method is used, which is superior to the classical trial and error method. The database covers a wide range of river width (0.2- 867m), and depths (0.034- 19.9 m). Fifteen different combinations of river width (B), depth (H), flow velocity (U) and shear velocity (U_*) are implemented as inputs to create fifteen estimative models. The output of the ANFIS-FFA model is compared with the ANFIS and previously published equations to check the performance of the proposed model. The results show that the highest accuracy is attained by the M1 model, with all geometric and hydrodynamic parameters as input variables in comparison with ANFIS and previous equations. The R^2 value, RMSE, MAE and NSE for ANFIS-FFA model are 0.67, 113.14 m^2/s, 48 m^2/s, and 0.63 for proposed dimensional model, and 0.35, 874.5, 520.8, and 0.1 in non-dimensional ANFIS-FFA model, respectively. These values were 0.37, 463.34 m^2/s, 85.69 m^2/s, and -5.19 for dimensional ANFIS model, and 0.11, 3269.88, 1932.09 and -11.54 for non-dimensional ANFIS model, respectively. Overall, hybridization caused 81%, 75%, 76% improvement in R^2, RMSE and MAE. In another contribution of the paper, by using the matrix form of developed ANFIS-FFA optimized parameters, a novel explicit calculation procedure for estimation of K_x is derived. Based on the results, the proposed ANFIS-FFA model exhibits significant improvements than the classical ANFIS and highlights that optimizing by nature-inspired optimization algorithms plays a critical role in strengthening the ANFIS estimations generality.

INDEX TERMS Longitudinal dispersion coefficient, ANFIS-FFA, maximum dissimilarity method, natural rivers, adaptive neuro-fuzzy inference system.

I. INTRODUCTION

Water is a necessary element in the world, for human life and survival. Most rivers are polluted nowadays, and these pollutants are transported in the river flow. River flow and pollutant transport studies are necessary for several applications such as analysis of water intake, sediment deposition, contamination control, and pollutant risk assessment [1]–[4]. The fundamental law of mass diffusion in water was first introduced by Fick (1855) [5] as $q = -D\frac{\partial c}{\partial x}$, where q is the mass flux of pollutant, D is the diffusion coefficient, and $\frac{\partial c}{\partial x}$ is the gradient of the mass concentration (c) in

The associate editor coordinating the review of this manuscript and approving it for publication was Yongming Li.

This work is licensed under a Creative Commons Attribution 4.0 License. For more information, see https://creativecommons.org/licenses/by/4.0/

x distance along the longitudinal direction [6], [7]. The diffusion coefficient is generally referred to the longitudinal dispersion coefficient [6], [8]. The injected pollutants are dispersed by advection and dispersion processes in longitudinal, vertical, and transverse directions [9], [10]. The longitudinal dispersion process becomes the main mechanism, when the mixing process in the lateral direction is fully developed [11], [12]. The longitudinal dispersion coefficient was first presented by Taylor [13], [14] as a measure of the one-dimensional dispersion process by the conventional advection-dispersion equation:

$$\frac{\partial C}{\partial t} + u\frac{\partial C}{\partial x} = K_x \frac{\partial^2 C}{\partial^2 x} \tag{1}$$

where C is the average of mass concentration in cross-section, t is the time, u is the velocity, x is the longitudinal coordinate, and K_x is longitudinal dispersion coefficient [15]. Fischer (1967) [16] developed the following integral expression [17] for K_x in rivers:

$$K_x = -\frac{1}{A}\int_0^B hu' \int_0^y \frac{1}{\varepsilon_t h} \int_0^y hu' dy\, dy\, dy \tag{2}$$

where A is the area of river cross-section, B is the river width, h is the flow depth, u' is the differences of the depth-averaged flow velocity at specified local y from average velocity over the cross-section of river, y is the location in the lateral direction, and ε_t is the local transverse mixing coefficient [9].

Longitudinal dispersion coefficient (K_x) has a significant effect on contaminants and mass transport in large rives [18]. Consequently, estimation of the longitudinal dispersion coefficient could be useful in the management of water quality in rivers and optimal pollution control strategies [19], [20]. Seo and Cheong [11] stated that the K_x is affected by three groups of factors, including hydraulic river features, vegetation, fluid properties and geometric patterns of river reach [21], [22]. The longitudinal dispersion coefficient measurements showed that the most effective parameters are channel width (B), flow depth (H), bed shear velocity (U^*) and cross-sectional average flow velocity (U) [23]. K_x can be expressed as the following functional expression:

$$K_x = f\left(H, B, U, U^*\right) \tag{3}$$

Several researchers tried to develop empirical and mathematical equations for calculating K_x based on Equation 2. The first researchers who investigated the theoretical method for estimation of K_x were Taylor [13], [14] and Fischer [16]. Also, Elder [24] studied the K_x in non-uniform flow and proposed the empirical equations. McQuivey and Keefer [25] integrated linear one-dimensional flow with dispersion equations for estimating K_x. Fischer [26], Liu [27], Iwasa [28] and Koussis and Rodriguez-Mirasol [29] accounted the impact of lateral flow velocity gradient on K_x and developed simple equations. Seo and Cheong [11] suggested a one-step regression method using hydraulic and geometric field data from 26 rivers for estimating K_x. Deng *et al.* [30] derived a theoretical equation of K_x for $\frac{B}{H} > 10$. Kashefipour and Falconer [31] also proposed two-step regression models for estimating K_x using 81 data sets measured in natural streams of the USA. Seo and Baek [19] and Papadimitrakis and Orphanos [32] extended several empirical equations for estimating K_x in various ranges of $\frac{B}{H}$ values. These equations have several limitations, such as narrow calibration data, a small range of applicability, non-generality of collected data, and weak estimates over unseen data. Furthermore, most of the reported empirical and theoretical equations were developed using particular assumptions and channels features. The performance of these equations changes broadly for their calibrated flow ranges and stream condition, and for smaller or more extensive ranges of flow have not accurate results [17], [33]. Hence, it is crucial to develop a model that would have an appropriate application in the global range of river and flow conditions.

Data-driven techniques for over a decade have been used to evaluate many hydraulic and hydrologic problems. Regarding the K_x estimation, the most frequently data-driven tools are ANN [17], [34], [35], ANFIS [15], [23], [36], genetic programming [37]–[39], SVM [36], [40], particle swarm optimization [41], differential evolution [42], Granular Computing Model [43], Polynomial regression [44] and regression kriging [18]. These studies are some of the recently published researches that have been widely carried out to estimate K_x based on a limited number of data and a small range of applicability. High accuracy and less uncertainty in K_x estimations have been observed using ANFIS technique in comparison with the other models and equations [15], [20], [23], [34], [39].

Recently, Nature-inspired optimization systems have been used in different fields of model optimization. In the field of artificial intelligence, these algorithms provide a solution to achieve improved performance of non-optimized models [45]. Firefly algorithm (FFA) is a novel meta-heuristic optimization algorithm that has provided the desired enhancement and improvement in the modeling accuracy. The FFA imitates the flashing behavioral patterns of fireflies [46] based on their frequency, duration, and brightness [45]. The FFA structure can effectively and simultaneously found the local and global optima in the dataset and solve multimodal optimization problems [47]–[50].

The FFA hybridized with ANFIS model is used to progress the accuracy of estimations, such as estimating the roller length of a hydraulic jump [51] and monthly streamflow forecasting [45]. These studies have proved that the FFA approach is able to eliminate the inaccuracy in estimation of extremely shallow stream flows. Furthermore, FFA have been used effectively in different studies such as estimating the minimum velocity in sewer pipes [52], [53], estimating field capacity and permanent wilting point in soil samples [54], forecasting electrical load [49], optimization of Van-Genuchten model parameters in soil-water characteristic curve [55] and selection of relevant attributes [56].

Their results have shown more robustness of FFA compared to the other optimization methods. The significant shortcomings of the previous studies over longitudinal dispersion estimation and the implemented methodologies are small range of used data, narrow calibration data, small range of applicability, non-generality of collected data, weak estimates over unseen data and ANFIS learning by mathematical methods. By considering all of these shortcomings, this research aims to provide further improvements for inferring the embedded mechanism in an extended database of K_x by hybridizing the nature-inspired algorithm FFA with traditional ANFIS. This will improve the accuracy of the ANFIS technique as it adjusts and optimizes the modeling parameters based on a global database of K_x. In this research, the functional form of equation (3) is used for developing a novel accurate methodology of ANFIS-FFA technique to estimate K_x in natural rivers based on a global database. Also, for the first time, SSMD is hybridized with the ANFIS-FFA for the best subset selection of the train and test sets. The observed K_x values of different worldwide rivers are collected and used for evaluating the fitness of models. The proposed ANFIS-FFA model presents the relation between K_x as output, and hydraulic and geometric parameters as inputs. There is no need for assumptions on the hydraulic and geometric parameters of flow in the ANFIS-FFA model. The rest of the paper is organized as follows: Section II represents the datasets and pre-processing, ANFIS, FFA, and hybrid models implemented in the simulations and evaluation criteria. Section III contains the results and discussions about the proposed model. Finally, in Section IV, the conclusions were drawn.

II. MATERIAL AND METHODS

A. LONGITUDINAL DISPERSION DATA COLLECTION

There is an extensive set of the hydrodynamic and geometric parameters affecting the K_x values in natural streams. Among all, channel width (B), flow depth (H), flow velocity (U), and bed shear velocity (U^*) strongly affect the K_x [20], [39]. U affects the driving force of flow and U^* increases the longitudinal transfer of pollutant. B and H are geometrical parameters of the river cross-section that define and magnify the transverse distribution of longitudinal flow components and produce transverse velocity gradients as the main agent of dispersion. Also, vertical mixing is related to the flow depth H and can affect the dispersion process. Both dimensional and non-dimensional combinations of these parameters have been used for K_x estimation in previous studies. As the dimensional value of K_x is utilized in practical applications and numerical models, in this paper, a dimensional estimation is carried out. For this purpose, a field data bank, including 503 data points from different worldwide rivers are collected from the literature [27], [30], [31], [57]–[69] (Appendix 1). Table 1 represents the statistical features of subsets, which are selected by SSMD (discussed in the next section). Table 1 shows that the river width varies from 0.2 to 867 meters, flow depth varies from 0.034 to 19.6 meters, and K_x varies from 0.005 to 1798.60 m^2/s, which declares the

TABLE 1. Statistical characteristics of the dataset variables (after Riahi-Madvar *et al.* 2019).

Data Set	Parameter	Min	Max	Mean	SD	Skewness	Kurtosis
Total (503 data)	B (m)	0.2	867	56.49	110.87	4.86	28.37
	H (m)	0.034	19.9	1.42	2.31	4.60	27.43
	U (m/s)	0.022	1.74	0.49	0.31	1.26	2.25
	U^*(m/s)	0.001	0.99	0.066	0.07	7.098	74.00
	K (m^2/s)	0.005	1798.60	71.56	191.99	5.55	36.85
Train (351 data)	B (m)	0.2	867	63.89	118.13	4.46	23.68
	H (m)	0.034	19.9	1.56	2.46	4.44	25.018
	U (m/s)	0.022	1.74	0.47	0.33	1.29	1.876
	U*(m/s)	0.001	0.99	0.07	0.08	7.07	69.49
	K (m^2/s)	0.004	1798.60	78.76	194.22	5.27	34.374
Test (152data)	B (m)	0.19	857	40.19	90.75	6.49	51.66
	H (m)	0.058	16.76	1.10	1.88	5.09	34.86
	U (m/s)	0.023	1.71	0.53	0.27	1.48	4.49
	U^*(m/s)	0.003	0.51	0.07	0.05	5.18	41.10
	K (m^2/s)	0.008	1490	54.71	186.92	6.47	46.04

generality of collected database and their extensive ranges. In this research, four variables, including B, H, U and U* are considered as input vector of the estimative models and K_x assigned as the output of the models. All possible combinations (fifteen) of four input variables are used. Fifteen different model structures were used, and analysis of the results were carried out to show the sensitivity of each parameter on the model output in the train, test and overall data. For this purpose, 15 possible input combinations that are represented in Table 2 are considered.

TABLE 2. Different input vector combinations used for ANFIS-FFA developments.

Model	input parameter(s)
1	B, H, U, U*
2	B, H, U
3	H, U, U*
4	B, H, U*
5	B, H
6	U,U*
7	B,U
8	B,U*
9	U,H
10	U*,H
11	B
12	U*
13	H
14	U
15	B,U,U*

B. DATA PRE-PROCESSING BY SSMD

For a robust estimation, it is necessary to calibrate and train the model appropriately by selecting a suitable training set. The training performance highly depends on the dataset that is utilized for train purpose. There is no unique method for selecting the training and testing datasets. Trial and error and cross-validation methods were used in subset selection in previous studies of artificial intelligence [15], [70], [71]. In this research, we explore a robust algorithm to divide data into subsets and extract proper training set. One of the main factors in train and test subset selection is that the statistical characteristics of both training and testing subsets must be approximately identical. For example, if the train subset does not include the extreme values, but the test subset has several extreme values, the model could not be able to accurately estimate the extreme values and vice versa. This reduces the global applicability of trained models. To remedy this problem, in this research, SSMD method [72] was used for finding optimum subsets and random data manipulation to categorize training and testing subsets. In general, the SSMD method is capable of selecting the training and testing subsets in such a way that the statistical characteristics of subsets, including the maximum, minimum, mean, and standard deviation are stable, which guarantee a reliable estimation. The SSMD was first introduced by Kennard and Stone (1969) [73]. Based on SSMD, the data with the highest dissimilarity to others in the data set are selected [74] to characterize the overall behavior of the dataset. To remove the scale effects, before subset selection, the data are normalized as follows [6]:

$$x_n = \frac{x_i - x_{\min}}{x_{\max} - x_{\min}} \tag{4}$$

Then subsets are de-normalize as:

$$x_i = x_n\left(x_{\max} - x_{\min}\right) + x_{\min} \tag{5}$$

In this research, 70% and 30% of the whole dataset are selected automatically by SSMD as training and testing subsets, respectively. For more details on the SSMD method, one can refer to [6], [7], [39], [73]–[76]. Table 1 represents the statistical features of selected subsets. Also, Figure 1 shows the distribution of selected subsets. From Table 1 and Figure 1, it can be concluded that the SSMD is capable of propagating the extreme values in training and testing subsets equally, which eliminates the trial and error subset selection and improve the applicability and reliability of estimations. Figure 1 shows that the scattering of the training subset contains the borders of the database, and the members of the testing subset are positioned within the training subset. Subsequently, it expects that the trained models with SSMD suitably can realize the outliers' behavior in the database. Based on the results in this figure, the changes of variables in the train subset are greater than the test subset, and this increase the generalization of extrapolation models. The critical distinctiveness of the SSMD is that it spreads the extreme values in the train and test sets and does not eliminate them from modeling. For a global database as used in this paper, The SSMD, by extending the cover limits of the train set, strengthens the global uses of established estimations.

As Figure 1 shows, although the training set includes the upper and lower limits of the database, also there are some extreme values in test sets, and both of the selected datasets have a uniform pattern of variables that avoids the overfitting of the model. Indeed by using the SSMD, the selection process is progressed in such a way that there will be maximum dissimilarity between the members of an individual set and the same values will not occur in one set.

C. ADAPTIVE NEURO-FUZZY INFERENCE SYSTEM (ANFIS)

The Fuzzy logic (FL) developed by Zadeh [77] is based on semantic uncertainty, which effectively used in various environmental and water resources problems [78]. Fuzzy inference system is a rule-based structure with three conceptual mechanisms, including a rule-based structure, a database of models and an inference system. The first component is based on if-then rules, while the second defines the membership function, and the third is the combination of the rules

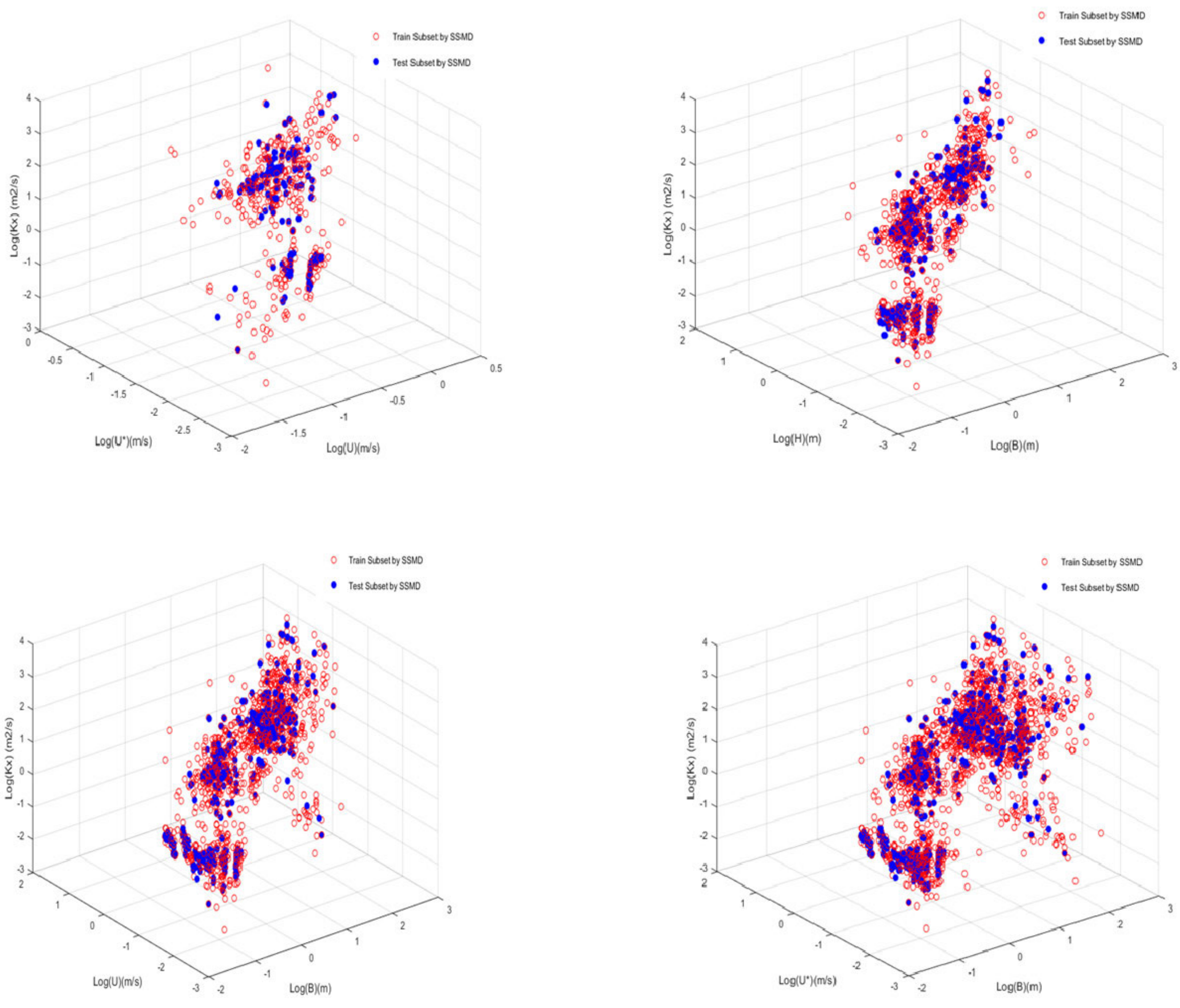

FIGURE 1. **The coverage and distribution of train and test subsets.**

and producing the results [79], [80]. An automatic procedure for the optimization of membership function features and adjusting parameters is needed [79], [81], [82]. ANFIS, which is the integration of fuzzy logic and artificial neural network (ANN) is used to overcome this problem [83], [84]. Generally speaking, ANFIS is a multi-layer feed-forward network based on the ANN learning capabilities and fuzzy thinking [79], [85]–[87]. Tsumoto, Mamdani and Sugeno are three categories of ANFIS, while the Sugeno is the most popular [88], [89] and used in this research. Also, there are several membership functions (including Trapezoidal, Gaussian, Sigmoid, Triangular, Generalized bell-shaped, etc.) for ANFIS [90]. The selection of the membership function is a crucial part of ANFIS modeling. A Sugeno first-order fuzzy model with four inputs and one output is described here to show how the ANFIS system works. In this research, geometric and hydrodynamic parameters of flow are the input and longitudinal dispersion coefficient (K_x) is the output variables. The rules for the ANFIS system are presented in equations (6) and (7):

Rule 1: IF H is A_1, U^* is B_1, U is C_1 and B is D_1 then

$$K_{X_1} = a_1 H + b_1 U^* + c_1 U + d_1 B + r_1 \tag{6}$$

Rule 2: IF H is A_2 and U^* is B_2, U is C_2 and B is D_2 then

$$K_{X_2} = a_2 H + b_2 U^* + c_2 U + d_2 B + r_2 \tag{7}$$

In which a_i, b_i, c_i and d_i are the parameters which would be optimized by the FFA during the training procedure, K_{xi} is the output of the fuzzy system, and A_i, B_i, C_i and D_i are the fuzzy sets. Figure 2 shows the schematic ANFIS model, which is used in this study. Based on Figure 2, there are five layers in ANFIS modeling, which briefly discussed here.

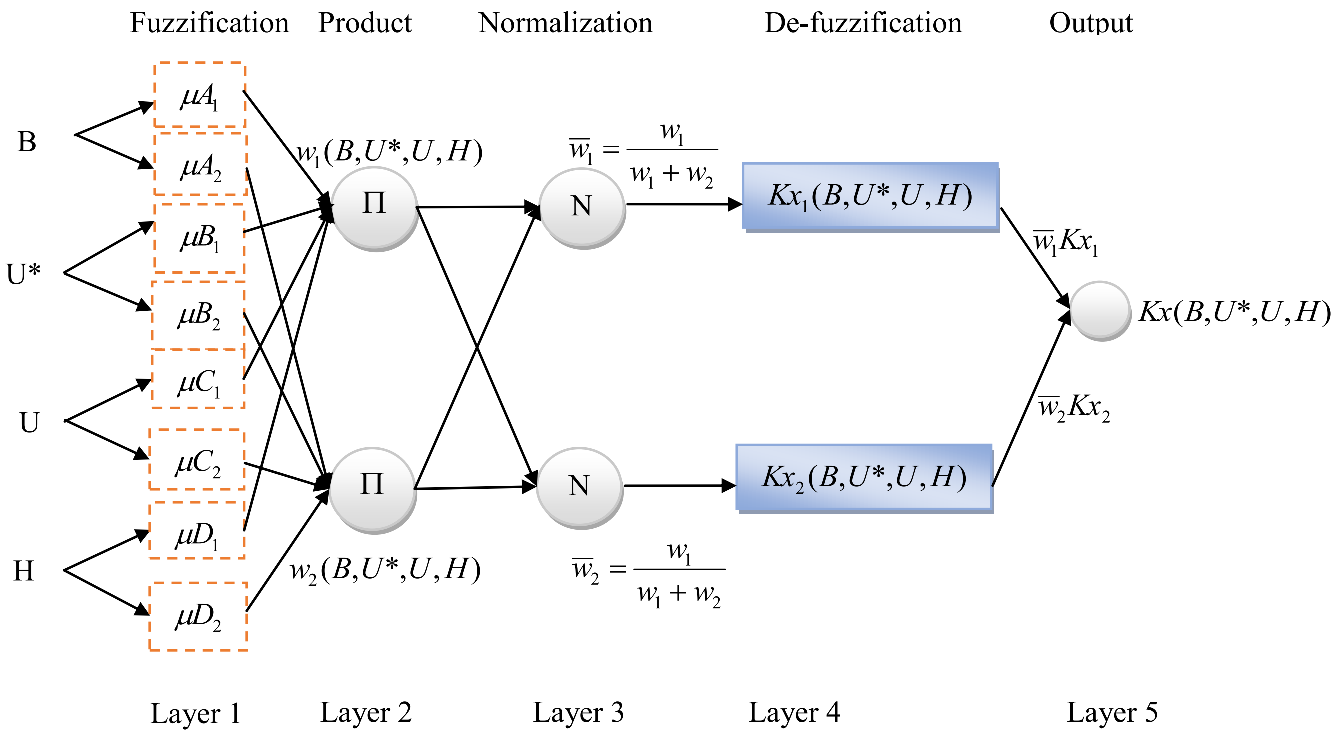

FIGURE 2. **The architecture of ANFIS in K_x estimation.**

Layer 1: The input layer adopts the activation function on input variables.

$$O_{1,i} = \mu_{Ai}(x) \quad for\ i = 1, 2,\ or$$
$$O_{1,i} = \mu_{Bi-2}(y) \quad \text{for } i = 3, 4 \tag{8}$$

where one of the B, H, U and U* is the input to each node and A_i or B_{i-2} is related linguistic label and $O_{1,i}$ is the membership grade of fuzzy sets. In this step, several membership functions are tested and finally, Gaussian membership function is used.

$$\mu_{Ai}(x, \sigma, c) = e^{\frac{-(x-c)^2}{2\sigma^2}} \tag{9}$$

In which σ and care membership function of variables set. So the output of the first layer is as follows:

$$O_{1,i=}\mu_{Ai}(x) = e^{\frac{-(x_i-c_i)^2}{2\sigma_i^2}} \tag{10}$$

Layer 2: This layer determines the membership degree of inputs.

$$O_{2,i} = \mu_{Ai}(x)\mu_{Bi}(y) \quad i = 1, 2 \tag{11}$$

Layer 3: This layer calculates the relative weights of inputs.

$$O_{3,i} = \bar{w}_i = \frac{w_i}{w_1 + w_2} \quad i = 1, 2 \tag{12}$$

Layer 4: This layer adopts inputs with relative weights.

$$O_{4,i} = \bar{w}_i K_{x_i} = \bar{w}_i(a_i H + b_i U^* + C_i U + D_i B + r_i) \tag{13}$$

Layer 5: This layer calculates the final output of the model.

$$O_{5,i} = \sum_i \bar{w}_i K_{x_i} = \frac{w_1 K_{x_1} + w_2 K_{x_2}}{w_1 + w_2} \tag{14}$$

In general, ANFIS has a high capability in learning and classifying input-output data. However, training the ANFIS model to obtain optimal membership function and parameters is time-consuming. So, in this research, The Firefly Optimization Algorithm (FFA) was utilized to solve this problem

D. FIREFLY ALGORITHM AND HYBRIDIZING ANFIS-FFA

In the present paper, the firefly optimization algorithm (FFA) was utilized to find the optimum values of parameters for the membership function. FFA was introduced by Yang [48], which is based on firefly behavior and flashing features. The mata-heuristic algorithms such as FFA need proper setting of parameters and need several iterations to find the optimal response. In reverse, faster convergence and low probability of entrapping in local optima are two main advantages of these algorithms.

The flashing features are categorized into three rules [48]:

- The fireflies assumed to be unisex and as a result, attracting to other fireflies is not based on the sex.
- The attractiveness is relative to the brightness and in the case that no one is brighter, the movement is random.
- The brightness is proportional to the light emission.

Based on these three rules, the brightness and the intensity of light emission can be the objective function [45]. The firefly

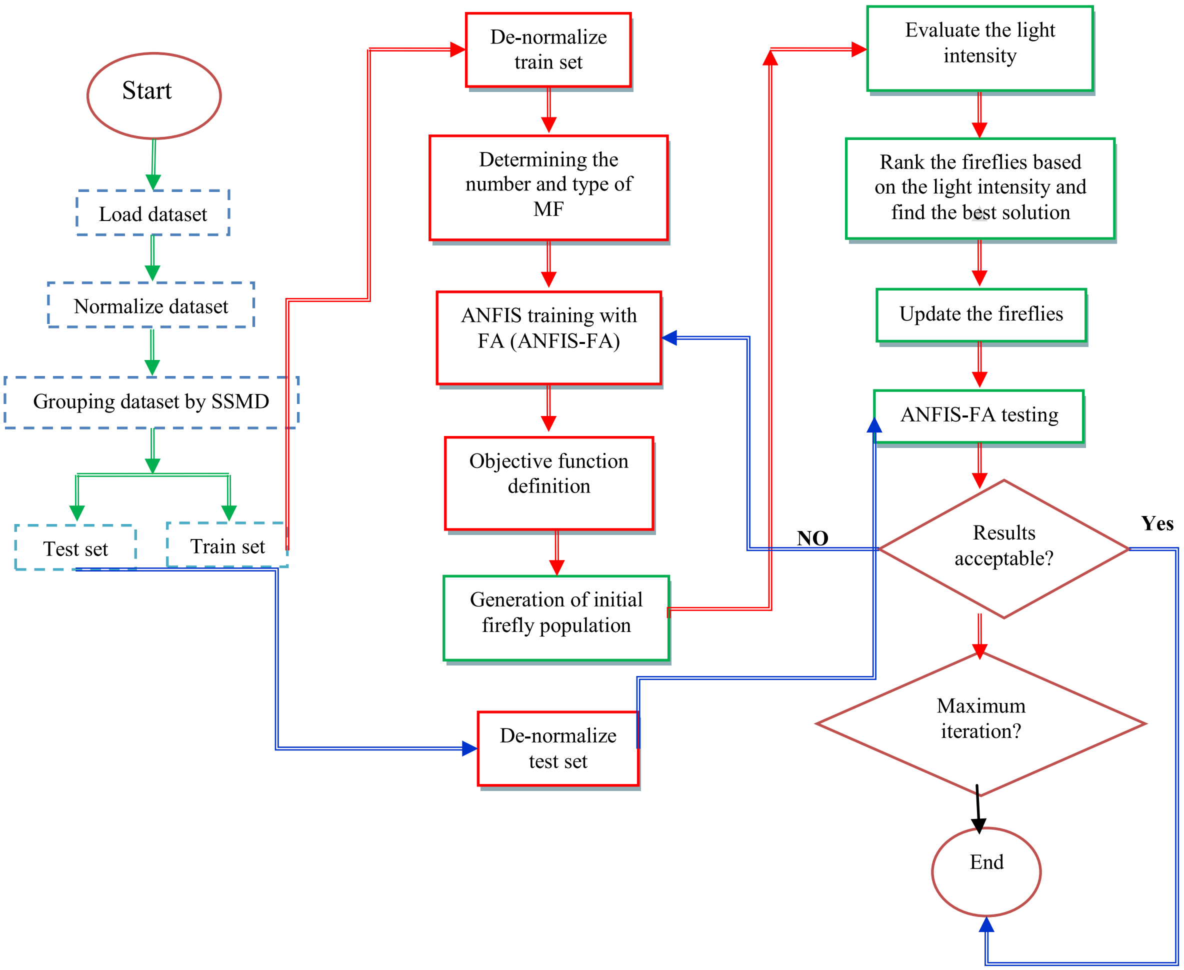

FIGURE 3. The flowchart of integrated SSMD with ANFIS-FA modeling.

light intensity and attractiveness were formulated as follows:

$$I = I_0 e^{-\gamma r}$$
$$\beta = \beta_0 e^{-\gamma r^2} \tag{15}$$

where I and β are firefly light intensity and attractiveness, respectively. I_0 and β_0 represent the original light intensity and attractiveness at r=0, r is the distance of two fireflies and γ is the light absorption coefficient. The Cartesian distance between two fireflies introduces as [48]:

$$r_{ij} = \left\| x_i - x_j \right\|_2 \tag{16}$$

The distance is not to be Cartesian distance and also can be the time delay and, etc. [48]. Also the movement of one firefly by another one is defined as [48]:

$$x_i = x_i + \beta_0 e^{-\lambda r_{ij}^2} \left(x_j - x_i\right) + \alpha \varepsilon_i \tag{17}$$

where α and ε_i are randomization coefficient (between 0 and 1) and random number vector, respectively [45].

In this paper, 15 models with different input variables that have only 1 output parameter of K_x are developed (Table 2). The ANFIS-FFA uses root-mean-square error (RMSE) as the cost function in the optimization of the ANFIS parameters. The limits of parameters that are optimized by the cost function in FFA should be identified first. In the hybrid optimization flowchart, as presented in Figure 3, each firefly includes a set of two types of optimization parameters, antecedent and consequent parameters given in equations 9, 10 and 13. In this paper in the M1 model, as the best one from 15 models, B, H, U and U* are used as input vector, and the associated output parameter (K_x) is estimated. If the input vector has three fuzzy membership functions of Gaussian MFs, then the IF–THEN rules can be written as:

Rule s: IF B is $F_1^i(s_{1i}, c_{1i})$ and H is $F_2^i(s_{2i}, c_{2i})$ and U is $F_3^i(s_{3i}, c_{3i})$ and U* is $F_4^i(s_{4i}, c_{4i})_1$ then

$$K_{xs} = a_s B + b_s H + c_s U + d_s U^* + r_s \tag{18}$$

The parameters of ANFIS that should be optimized are (s_{ji}, c_{ji}, a_s, b_s, c_s, d_s, r_s) and these parameters are decision variables in the optimization problem. These parameters for all of the associated rules and MFs need to be determined. The primary firefly population is selected randomly, and each firefly is imagined into the ANFIS parameters set. According to each firefly's light intensity, the attractiveness (cost) of each firefly (ANFIS parameter) is calculated and assessed, and fireflies (parameter values) with the lowest light move toward parameters with the highest cost (brightness). Consequently, the cost function is calculated. The cost function in this paper is the minimization of root mean square error (RMSE) of estimations in regard to decision variables. This procedure cycles until the maximum generation value or minimum preferred cost function are derived. Figure 3 shows the flowchart of hybrid SSMD with ANFIS–FFA that is used in this paper to estimate K_x.

E. EVALUATION CRITERIA

There are several statistical performance evaluation criteria for model assessment. In this paper, eight statistical evaluation criteria, including the root mean square error (RMSE), the coefficient of determination (R^2), mean absolute error (MAE), the Nash-Sutcliffe Efficiency (NSE), index of agreement (d), persistence index (PI), confidence index (CI) and relative absolute error (RAE) were utilized for model evaluation. The explanation of these criteria was presented elsewhere [80], [91], [92]. Also, visualize approaches, including scatter plot, Taylor diagram [93], ellipse confidence bounds, and the probability distribution of revised discrepancy ratio (RDR) are used to evaluate the model results.

Beside these criteria, a revised discrepancy ratio (RDR) was used. Discrepancy ratio (DR) was introduced by White *et al.* [94] to examine the model robustness:

$$DR = Log\left(\frac{\text{Predicted Value}}{\text{Observed Value}}\right) \tag{19}$$

However, this form of DR is not applicable to zero or negative values. Noori *et al.* [95] proposed a new index (DDR) based on the DR to remedy this problem. However, the logarithmic base of the DR is eliminated in DDR:

$$DDR = \frac{Forecasted\ Value}{Observed\ Value} - 1 \tag{20}$$

Because of these shortcomings, RDR was proposed by Memarzadeh *et al.* [76] as a new index which is capable of using for all negative, positive values and the logarithmic base of DR remains and calculates the normalized error of estimated values as follows:

$$RDR = Sign\,(\text{Estimated}.K_x - \text{Measured}.K_x) \times \left|\log\left|\frac{\text{Estimated}.K_x}{\text{Measured}.K_x}\right|\right| \tag{21}$$

In the case of over estimation of model results, the value of RDR >0, in the case of underestimation, RDR<0, and for exact estimations, RDR is equal to zero.

III. RESULTS AND DISCUSSION

The results of ANFIS-FFA and previously published equations are presented in this section. To evaluate the results of models and compare their capability versus existing equations, some graphical and statistical indices are used. In next subsection the results of ANFIS-FFA with different input parameters and comparing the best ANFIS-FFA model with existing equations are presented respectively.

A. RESULTS OF ANFIS-FFA MODEL

The ANFIS model is trained by Firefly Algorithm using 503 data points, which are collected from previously published data. The SSMD approach is used to select the training and testing data subset of models, as described previously. The 351 number of K_x values contains the training data set, whereas 152 remaining ones are used in the testing stage. The primary comparative analysis in this research shows that the input vector in the dimensional state is superior to dimensionless values. So in this research, the dimensional parameters of U(m/s), U*(m/s), B(m) and H(m) were used. The input layer of the ANFIS model has a different combination of these 4 parameters, and by this way, 15 models are trained using FFA. The output layer of ANFIS-FFA includes a single variable as K_x. As described previously in the ANFIS structure, each input parameter has several parameters in terms of rules, and furthermore, each rule contains several parameters of membership functions. The membership function type, the number of clusters, and type of FIS are determined by trial and errors. It was found that the best is the Gaussian membership function with two parameters, 8 clusters (number of membership functions for each variable) and genfis3. In this research, the FIS structure (genfis3) is of the specified type, Sugeno and 8 numbers of clusters to be generated by fuzzy c-means (FCM) clustering. The input and output membership function types are ‘gaussmf’ and ‘linear’, respectively. The symmetric Gaussian function depends on two parameters sigma and c (Eq.10). The linear output function has 5 parameters (Eq. 13). So the input parameters that should be determined are 4. In this research, each parameter has 8 rules (membership functions), and each rule contains 2 parameters. In the largest input vector, there are 64 (4 variable $\times$8 rules $\times$ 2 parameters) parameters that must be optimized by the firefly algorithm in layer 2. In layer 3, this combination produces 4^8 nodes and in layer 5, there are $2^3\times5$ unknown parameters within the de-fuzzifcation process. So, we have 104 ANFIS parameters that should be determined and optimized by the firefly algorithm. In other cases with a reduced number of input variables (Table 2), the numbers of optimization parameters are reduced proportionally.

In this paper, all possible combinations of U, U∗, B and H variables are used (Table 2). The FFA is used in all 15 combinations of input vector (Table 2) for the optimization of ANFIS parameters over the training data set selected by SSMD. In Figure 4, the variation of the best cost function with generations in the M1 model of ANFIS-FFA is shown. It shows the trend of cost reduction as a function of iteration over the firefly optimization process, and it was found that after 500 generations, the best solution was achieved and the model converged to the optimized parameters of ANFIS. The final results of 15 ANFIS-FFA models are summarized in Figures 5-9 and Tables 3-5. Figure 5 visualizes the Taylor diagram of K_x estimated by ANFIS-FFA with different input parameters in the train, test and overall of the data. The Taylor diagram visually compares the quantitative performance of 15 ANFIS-FFA models for the train, test and all

TABLE 3. Results of ANFIS-FFA models for estimation of K_x over training data.

	M1	M2	M3	M4	M5	M6	M7	M8	M9	M10	M11	M12	M13	M14	M15
RSQ	**0.72**	**0.76**	**0.71**	0.62	0.61	**0.70**	0.56	0.63	0.53	**0.71**	0.42	0.31	0.28	0.53	0.76
RMSE(m^2/s)	**102.25**	**95.34**	**104.47**	119.72	121.49	**106.61**	128.90	117.06	131.97	**103.42**	147.69	160.77	164.16	132.66	95.16
MAE	**51.42**	**49.11**	**56.65**	54.46	56.28	**60.61**	59.43	52.95	60.09	**53.84**	63.79	85.05	74.95	68.80	44.58
PI	**0.86**	**0.88**	**0.86**	0.81	0.81	**0.85**	0.79	0.82	0.77	**0.86**	0.72	0.67	0.65	0.77	0.88
RAE	**0.52**	**0.50**	**0.57**	0.55	0.57	**0.61**	0.60	0.54	0.61	**0.54**	0.65	0.86	0.76	0.70	0.45
d	**0.91**	**0.92**	**0.91**	0.87	0.86	**0.90**	0.84	0.88	0.82	**0.91**	0.74	0.66	0.63	0.82	0.93
NSE	**0.72**	**0.76**	**0.71**	0.62	0.61	**0.70**	0.56	0.63	0.53	**0.71**	0.42	0.31	0.28	0.53	0.76
CI	**0.66**	**0.70**	**0.64**	0.53	0.52	**0.63**	0.46	0.55	0.44	**0.65**	0.31	0.20	0.18	0.44	0.70

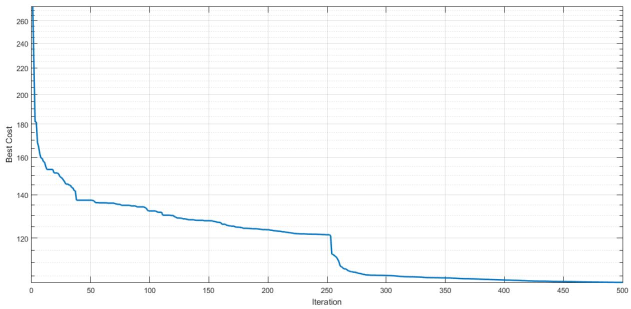

FIGURE 4. Convergence process and best cost variations of ANFIS-FFA over generation.

of the data. This figure evaluates the quantitative accuracy of ANFIS-FFAs comparatively and shows that the nearest estimations to the observed values of K_x are reproduced in M1. As it is expected, the models with one or two inputs had the worst performance.

Tables 3-5 shows that by increasing the number of input parameters, the model result improved. The R^2 values of the M1 model in the train, test and overall data are 0.72, 0.67 and 0.7, respectively and MAE values are 51.72, 48, 50.6 and NSE are 0.72, 0.63 and 0.7, respectively. These values show the superiority of the M1 model over the others. Figure 6 shows the RDR distribution of the best 6 models in the test step, including M1, M2, M5, M7, M9 and M14, and M1, M2, M4, M5 M6 and M7 for overall data. In these graphs, further inclination in RDR spreading to the centerline and higher values of the maximum RDR are related to more accuracy. Based on this figure, the selected models in regard to RDR have some positive skewness, but in comparison with wide ranges of input and output values in Table 1, the overall performances are valuable.

Observed and predicted K_x and associated errors in the training and testing steps for M1 using ANFIS-FFA are drawn in Figures 7 and 8, respectively. It is noticeable that the estimated and measured values have the same trends, and the measured and estimated K_x values have approximately similar patterns. The model estimations are accurate, particularly at small or large K_x values, and have an acceptable correlation with measurements. From these figures, it is finding out that ANFIS-FFA accurately can inference the inherent relationships between four hydraulic and geometric features of natural rivers (U, U_*, B, H) with K_x. It must be noted that the main aim of the research was to improve ANFIS capabilities in

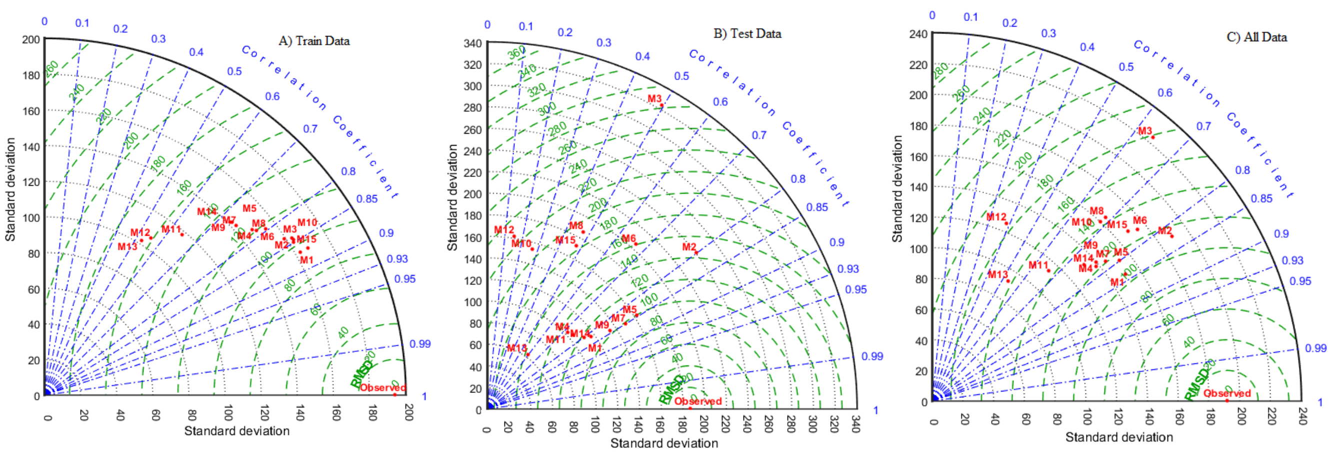

FIGURE 5. Taylor diagram for training, testing and overall data for all combinations of variables in ANFIS-FFA.

TABLE 4. Results of ANFIS-FFA models for estimation of K_x over testing data.

	M1	M2	M3	M4	M5	M6	M7	M8	M9	M10	M11	M12	M13	M14	M15
RSQ	**0.67**	**0.64**	0.24	0.57	**0.71**	0.44	**0.72**	0.22	**0.71**	0.07	0.52	0.02	0.35	**0.64**	0.23
RMSE(m^2/s)	**113.14**	**146.63**	285.55	127.55	**100.05**	162.49	**98.63**	191.73	**104.04**	207.65	132.88	231.15	157.53	**118.93**	183.80
MAE	**48.00**	**45.99**	75.63	42.28	**39.99**	61.78	**36.99**	58.03	**44.08**	63.82	45.18	103.24	52.52	**60.80**	49.22
PI	**0.82**	**0.70**	-0.13	0.77	**0.86**	0.63	**0.86**	0.49	**0.85**	0.40	0.75	0.26	0.66	**0.80**	0.53
RAE	**0.66**	**0.63**	1.04	0.58	**0.55**	0.85	**0.51**	0.80	**0.61**	0.88	0.62	1.42	0.72	**0.84**	0.68
d	**0.85**	**0.87**	0.60	0.78	**0.91**	0.80	**0.91**	0.64	**0.89**	0.42	0.76	0.30	0.54	**0.83**	0.64
NSE	**0.63**	**0.38**	-1.35	0.53	**0.71**	0.24	**0.72**	-0.06	**0.69**	-0.24	0.49	-0.54	0.28	**0.59**	0.03
CI	**0.53**	**0.33**	-0.81	0.42	**0.65**	0.19	**0.65**	-0.04	**0.61**	-0.10	0.37	-0.16	0.15	**0.49**	0.02

TABLE 5. Results of ANFIS-FFA models for estimation of K_x over all data.

	M1	M2	M3	M4	M5	M6	M7	M8	M9	M10	M11	M12	M13	M14	M15
RSQ	0.69	0.68	0.41	0.59	0.63	0.59	0.60	0.47	0.57	0.47	0.43	0.16	0.28	0.54	0.57
RMSE(m^2/s)	107.70	115.08	180.21	123.92	117.40	127.69	122.47	145.06	126.05	144.34	144.96	185.85	163.56	130.42	129.97
MAE	51.43	49.21	63.36	51.85	52.45	62.00	53.76	5`5.51	56.34	57.86	59.26	91.53	69.28	67.45	47.01
PI	0.85	0.83	0.58	0.80	0.82	0.79	0.80	0.72	0.79	0.73	0.73	0.55	0.65	0.78	0.78
RAE	0.55	0.53	0.68	0.55	0.56	0.66	0.57	0.59	0.60	0.62	0.63	0.98	0.74	0.72	0.50
d	0.90	0.90	0.78	0.85	0.88	0.87	0.86	0.81	0.84	0.81	0.75	0.56	0.62	0.83	0.86
NSE	0.69	0.64	0.12	0.59	0.63	0.56	0.60	0.43	0.57	0.44	0.43	0.07	0.28	0.54	0.54
CI	0.62	0.58	0.10	0.50	0.55	0.49	0.51	0.35	0.48	0.35	0.32	0.04	0.17	0.45	0.47

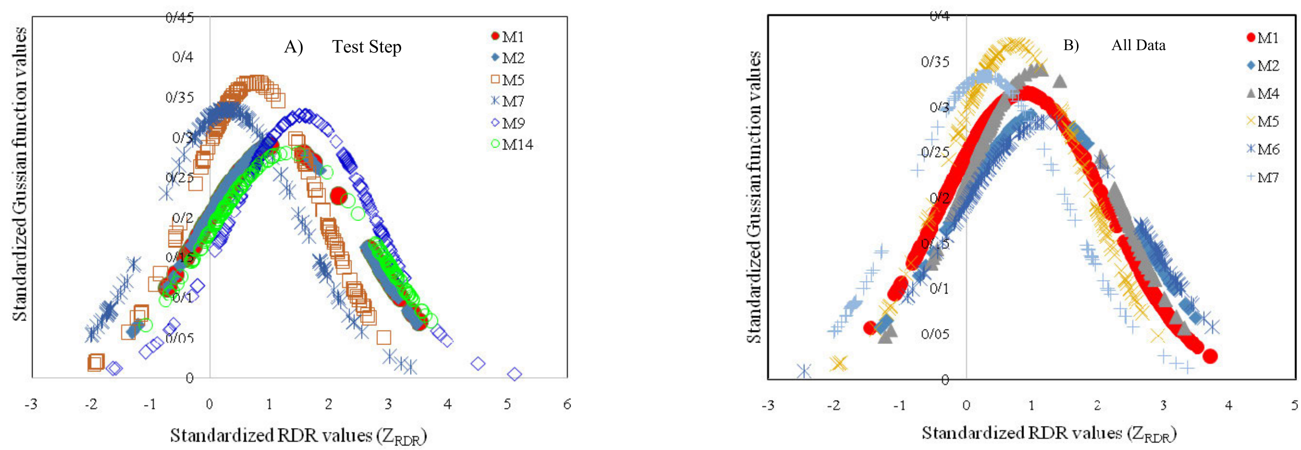

FIGURE 6. RDR values for the best ANFIS-FFA models using A) test and B) all of the data.

global conditions of natural rivers without clustering the data based on variable ranges, where will reduce the generality of estimation model and causes the over fitting challenges in artificial model estimations.

Figure 9 shows the regression plots of the ANFIS-FFA estimation versus the measured K_x values in the training, testing steps and all of dataset. The correlation coefficient (R), as an index of the linear correlation between the estimated and measured K_x, was calculated and presented for M1 using the ANFIS-FFA model in these figures. The results show acceptable agreement with the high R (0.84 and 0.85) and the 95% confidence ellipse of estimations. The blue points are those beyond the 95% bound of observations, and the green points are those inside the 95% confidence bound. From Figure 9, it is clear that in train step, 17 points of 352 number of observations (4.8%), in test step, 5 of 151 (3.3%) and over all data, 22 of 503 (4.4%) estimations are outside of the 95% ellipse bounds. It is concluded that the M1 model

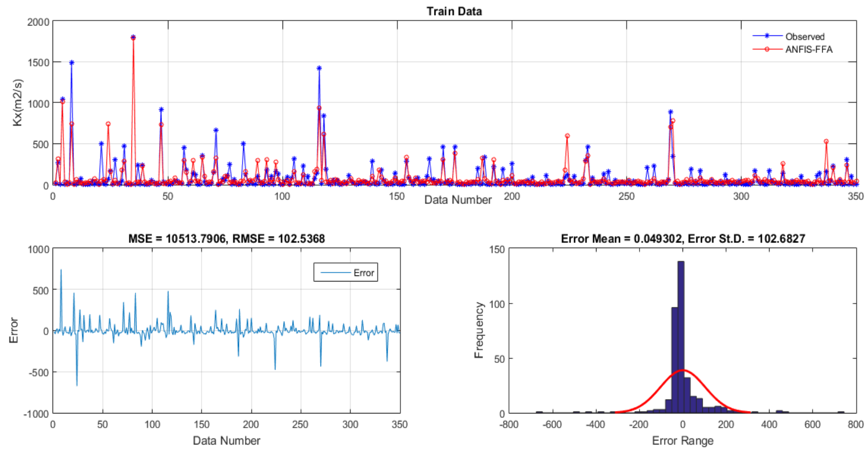

FIGURE 7. Comparing observed K_x versus predicted M1 ANFIS-FFA in train phase.

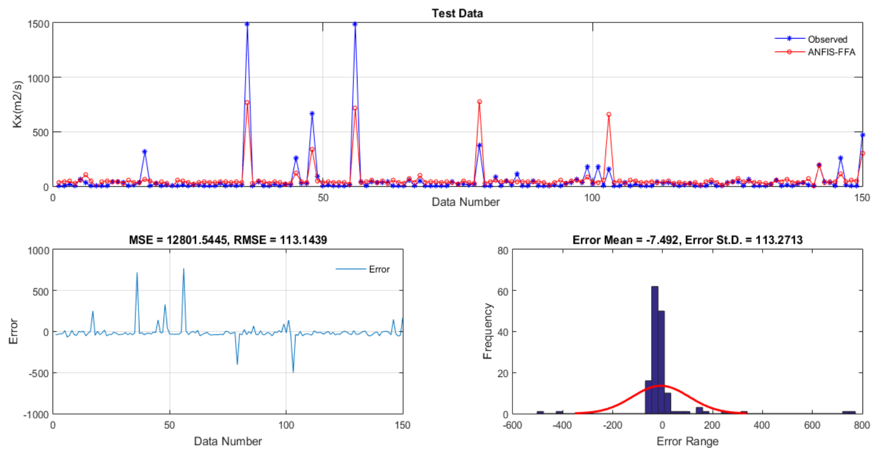

FIGURE 8. Comparing observed K_x versus predicted M1ANFIS-FFA in the test phase.

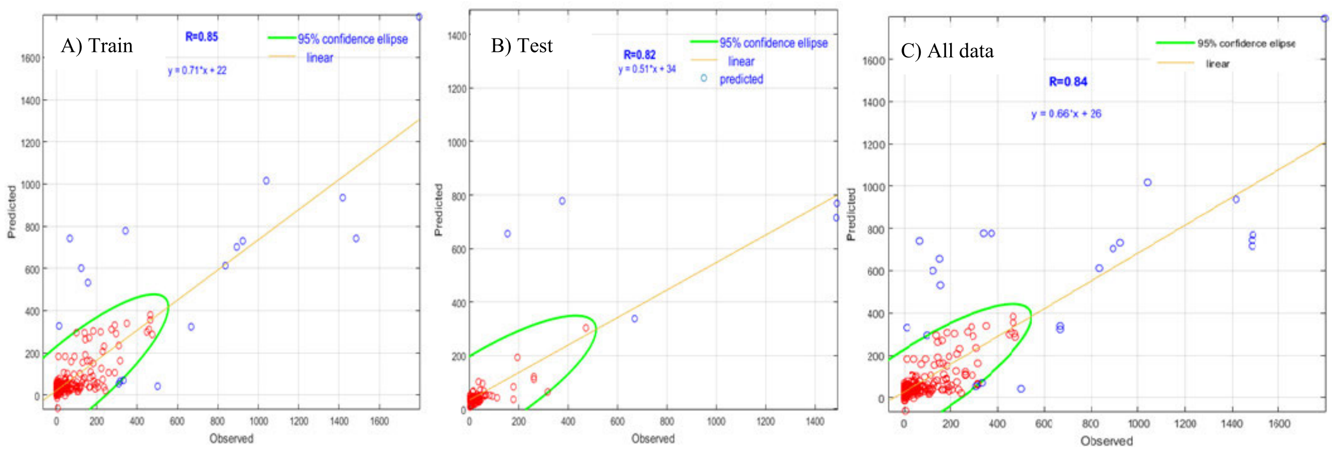

FIGURE 9. Scatter plot of observed Kx versus ANFIS-FFA predictions and 95% confidence ellipse for the best-selected model.

in ANFIS-FFA shows a satisfactory relationship between the estimated and observed K_x for most of the data points and the greatest part of the data points placed alongside the imagined unique line. Indeed, it is realized that in M1 using ANFIS-FFA, the number of both overestimation or underestimation of K_x is limited. Therefore, it is apparent that the K_x estimated by ANFIS-FFA benefits from the uppermost level of accuracy.

TABLE 6. Empirical equations used in K_X estimations.

Model	Formula
Fischer (1975)	$K_x = .011\left(\frac{U}{U^*}\right)^2\left(\frac{B}{H}\right)^2 HU^*$
Liu (1977)	$K_x = .18\left(\frac{U}{U^*}\right)^{0.05}\left(\frac{B}{H}\right)^2 HU^*$
Seo and Cheong (1998)	$K_x = 5.92\left(\frac{U}{U^*}\right)^{1.43}\left(\frac{B}{H}\right)^{.62} HU^*$
Deng et al. (2002)	$K_x = \frac{0.15}{8\varepsilon_t}\left(\frac{U}{U^*}\right)^2\left(\frac{B}{H}\right)^{1.67} HU^*$ $\varepsilon_t = 0.145 + \frac{\left(\frac{U}{U^*}\right)\left(\frac{B}{H}\right)^{1.38}}{3520}$
Kashefipour and Falconer (2002)	$K_x = 10.612\left(\frac{U}{U^*}\right)^2 HU^*$ For $\frac{B}{H} > 50$ $K_x = \left[7.428 + 1.775\left(\frac{B}{H}\right)^{.62}\left(\frac{U}{U^*}\right)^{.572}\right]\left(\frac{U}{U^*}\right)^2 HU^*$ For $\frac{B}{H} < 50$
Sattar and Gharabaghi (2015)	$K_x = 8.45\left(\frac{U}{U^*}\right)^{1.65}\left(\frac{B}{H}\right)^{0.5-0.514F_r^{0.516}+\frac{U}{U^*}0.42^{\frac{U}{U^*}}} HU^*$
Wang et al. (2017)	$K_x = \left(0.718 + 47.9\frac{H}{B}\right)\left(\frac{U}{U^*}\right)\left(\frac{B}{H}\right)HU^*$
Alizadeh et al. (2017)	$\frac{K}{HU^*} = 5.319\left(\frac{U}{U^*}\right)^{0.075}\left(\frac{B}{H}\right)^{1.206}$ For $\frac{B}{H} \le 28$ $\frac{K}{HU^*} = 9.931\left(\frac{U}{U^*}\right)^{1.802}\left(\frac{B}{H}\right)^{0.187}$ For $\frac{B}{H} > 28$

B. COMPARING ANFIS-FFA WITH ANFIS AND EMPIRICAL EQUATIONS

To evaluate the robustness of the ANFIS-FFA model in regard to empirical equations, the K_x was calculated for the test and all of the data using eight formulas that were developed in previous studies. The empirical equations are presented in Table 6. Also, the ANFIS model is developed to compare its results with ANFIS-FFA. A comprehensive evaluation of the M1 results by ANFIS-FFA with results of equations and conventional ANFIS over the test and all of the dataset are presented in Tables 7 and 8 for both dimensional and non-dimensional results. Indeed, these tables present the values of the statistical indices used to validate the applicability of published existing equations in estimating K_x for extended data from small to large rivers. The best results that are presented in Tables 7 and 8 are for equation Alizadeh *et al.* [41] with $R^2 = 0.20$, NSE=0.17 in test data and $R^2 = 0.16$, NSE $= -0.02$ over all of the data, respectively in dimensional results. In the Non-dimensional values, the best results are derived by the Seo and Cheong [11], equation with $R^2 = 0.37$ and NSE $= -0.32$ in the test set and $R^2 = 0.24$ and NSE $= -0.38$ over all of the data. These values show the limitation and weakness of empirical equations in the new database of K_x. After that, the equations of Sattar and Ghorbani [38] and Kashefipour and Falconer [31] have more accurate estimations for dimensional values among the existing K_x equations and have better results in comparison with the Seo and Cheong [11], Wang *et al.*, Fischer [26] and Deng *et al.* [30] equations. However, all of these equations have very low accuracy and high error than the ANFIS-FFA and ANFIS. The estimated values represented in these tables show that the collected data are very global, general and scattered, in such a way that nearly all of the equations have high error, and even the best equations do not yield reasonable estimations of K_x. According to these results, the ANFIS-FFA model is superior to the existing equations and conventional ANFIS model. In ANFIS model, the statistical parameters for the test step are $R^2 = 0.37$, RMSE $= 463.34$, MAE=85.69,

TABLE 7. Results of equations for estimation of K_x over testing data.

Parameters	Statistics	Fischer (1975)	Liu (1977)	Seo and Cheong (1998)	Deng et al. (2002)	Kashefipour and Falconer (2002)	Sattar and Gharabaghi (2015)	Alizadeh et al. (2017)	Wang et al. (2017)	ANFIS	ANFIS-FFA
Dimensional Values	R^2	0.22	0.19	0.22	0.35	0.14	0.15	0.20	0.24	0.37	**0.67**
	RMSE(m^2/s)	1685.56	169.31	575.47	1008.02	687.33	516.97	169.14	198.92	463.34	**113.14**
	MAE	275.05	44.00	92.15	628.76	234.62	87.34	55.40	50.88	85.69	**48.00**
	PI	-38.49	0.60	-3.60	-13.12	-5.57	-2.71	0.60	0.45	-1.98	**0.82**
	RAE	3.78	0.60	1.27	8.64	3.22	1.20	0.76	0.70	1.18	**0.66**
	d	0.18	0.50	0.40	0.30	0.31	0.37	0.58	0.65	0.54	**0.85**
	NSE	-80.95	0.17	-8.55	-28.31	-12.63	-6.71	0.17	-0.14	-5.19	**0.63**
	CI	-14.24	0.09	-3.42	-8.62	-3.93	-2.51	0.10	-0.09	-2.79	**0.53**
Non-Dimensional Values	R^2	0.26	0.15	0.37	0.001	0.03	0.15	0.01	0.16	0.11	**0.35**
	RMSE	5836.35	934.24	1060.62	53123.56	8862.50	1054.34	1418.09	870.93	3269.88	**874.50**
	MAE	1516.55	365.90	638.99	30357.72	5382.46	666.86	975.77	541.76	1932.09	**520.80**
	PI	-18.91	0.49	0.34	-1648.46	-44.91	0.35	-0.18	0.56	-5.25	**0.55**
	RAE	3.36	0.81	1.42	67.27	11.93	1.48	2.16	1.20	4.28	**1.15**
	d	0.25	0.56	0.71	0.01	0.03	0.57	0.24	0.51	0.34	**0.73**
	NSE	-38.96	-0.02	-0.32	-3309.36	-91.13	-0.30	-1.36	0.11	-11.54	**0.10**
	CI	-9.92	-0.01	-0.23	-35.13	-2.57	-0.17	-0.32	0.06	-3.96	**0.07**

TABLE 8. Results of equations for estimation of K_x over all data.

Parameters	Statistics	fisher 1975	Liu 1977	Seo and Cheong (1998)	Kashefipour and Falconer (2002)	Sattar and Gharabaghi (2015)	Wang et al. (2017)	Alizadeh et al. (2017)	Deng et al. (2002)	ANFIS	ANFIS-FFA
Dimensional Values	R^2	0.03	0.05	0.17	0.01	0.11	0.20	0.16	0.10	0.12	**0.69**
	RMSE(m^2/s)	6248.99	273.47	594.01	2334.09	541.67	214.27	194.71	1751.11	323.86	**107.70**
	MAE	760.85	73.20	132.68	526.90	117.46	66.86	72.80	941.77	67.33	**51.43**
	PI	0.51	0.51	0.51	0.51	0.51	0.51	0.51	0.51	-0.39	**0.85**
	RAE	8.24	0.79	1.44	5.70	1.27	0.72	0.79	10.19	0.73	**0.55**
	d	0.02	0.38	0.37	0.04	0.34	0.62	0.58	0.13	0.48	**0.90**
	NSE	-1061.96	-1.04	-8.60	-147.30	-6.99	-0.25	-0.03	-82.47	-1.86	**0.69**
	CI	-21.77	-0.40	-3.17	-6.21	-2.37	-0.16	-0.02	-10.91	-0.89	**0.62**
Non-Dimensional Values	R^2	0.21	0.18	0.24	0.001	0.04	0.22	0.08	0.08	0.30	**0.58**
	RMSE	634057.13	11631.18	3814.20	86063.96	3331.35	2874.61	3491.63	190431.23	2715.07	**2108.27**
	MAE	42067.93	1769.93	1379.35	11897.21	1267.98	950.54	1455.22	62288.78	987.23	**783.95**
	PI	0.52	0.52	0.52	0.52	0.52	0.52	0.52	0.52	0.52	**0.52**
	RAE	32.61	1.37	1.07	9.22	0.98	0.74	1.13	48.29	0.77	**0.61**
	d	0.01	0.34	0.65	0.00	0.32	0.55	0.47	0.02	0.66	**0.85**
	NSE	-38012.63	-11.79	-0.38	-699.37	-0.05	0.22	-0.15	-3427.93	0.30	**0.58**
	CI	-354.61	-4.00	-0.25	-2.83	-0.02	0.12	-0.07	-75.08	0.20	**0.49**

$NSE = -5.19$, and CI $= -2.79$ and for all of the data are $R^2 = 0.41$, RMSE=259.68, MAE=48.43, NSE $= -0.84$, and CI $= -0.59$ for the M1 which show the low accuracy in estimations by the ANFIS in comparison with the ANFIS-FFA. According to the results, comparing ANFIS with ANFIS-FFA, ANFIS-FFA in M1 has the highest accuracy. This result and the superiority of ANFIS-FFA versus ANFIS were approved by Azimi *et al.* [51] in calculating the roller length of a hydraulic jump on a rough channel bed. Also, Yaseen *et al.*, [45] stated the ANFIS-FFA model shows higher accuracy in results over than the non-optimized ANFIS model in forecasting the streamflow. Therefore, new strengthen models such as ANFIS-FFA are capable of estimating K_x precisely and can be implemented in pollution modeling.

After all the aforementioned quantitative and graphical evaluations, the superiority of the hybridized ANFIS-FFA model in estimating of K_x is distinct and can combine with numerical pollutant modeling.

TABLE 9. Gaussian parameters for weights calculation in eq. 22, optimized by ANFIS-FFA, with an example calculation.

									Output MFs= $exp[-\left(\frac{(X_i-c_j)^2}{2\sigma_j^2}\right)]$				$Pj=\prod_{j=1}^{4} OMf_j$	Relative Weight $w_j=\frac{P_j}{\sum_{j=1}^{8} P_j}$
	B(m)		H(m)		U(m/s)		U*(m/s)							
mf_j	Sigma	c	Sigma	c	Sigma	c	Sigma	c	B=53.3	H=2.09	U=0.79	U*=0.11	Pj	Wj
mf1	35.70	309.90	-1.48	-1.82	1.13	2.11	0.04	0.18	6.24E-12	3.05E-02	5.05E-01	1.43E-01	1.38E-14	4.14E-04
mf2	185.30	-808.90	6.62	-8.61	3.07	12.13	-0.06	-0.84	1.99E-05	2.71E-01	1.69E-04	3.31E-50	3.02E-59	9.08E-49
mf3	50.24	78.73	-0.01	0.34	-0.26	-1.57	0.11	0.35	8.80E-01	0.00E+00	1.29E-18	9.07E-02	0.00E+00	0.00E+00
mf4	-296.40	-211.50	-2.39	-24.60	0.90	0.95	0.00	0.52	6.71E-01	8.31E-28	9.84E-01	0.00E+00	0.00E+00	0.00E+00
mf5	90.50	-816.60	1.74	35.00	1.46	2.54	-0.15	-0.68	3.57E-16	2.09E-78	4.88E-01	4.66E-07	1.69E-100	5.09E-90
mf6	326.10	936.20	1.23	3.81	-0.13	-6.33	0.26	-1.17	2.56E-02	3.72E-01	0.00E+00	5.46E-06	0.00E+00	0.00E+00
mf7	-132.20	31.93	-1.36	-0.45	-0.42	2.17	-0.08	-0.36	9.87E-01	1.74E-01	4.53E-03	4.29E-08	3.32E-11	1.00E+00
mf8	-775.50	-2301.10	-0.20	4.85	0.11	-6.64	0.00	-0.58	9.95E-03	9.56E-01	0.00E+00	0.00E+00	0.00E+00	0.00E+00
												Sum	3.33E-11	

$$\mathrm{Out.mf(B)} = \mathrm{EXP}[-\left(\frac{(53.3-309.9)^2}{2(35.7^2)}\right)] = 6.24\mathrm{E}-12;\ \mathrm{Out.mf(H)} = \mathrm{EXP}[-\left(\frac{(2.09+1.82)^2}{2(-1.48^2)}\right)] = 3.05\mathrm{E}-2;$$

$$\mathrm{Out.mf(U)} = \mathrm{EXP}[-\left(\frac{(0.79-2.11)^2}{2(1.13^2)}\right)] = 5.05\mathrm{E}-1;\ \mathrm{Out.mf(U*)} = \mathrm{EXP}[-\left(\frac{(0.11-0.18)^2}{2(0.04^2)}\right)] = 1.38\mathrm{E}-14$$

TABLE 10. Consequent parameters in the estimative equation of Kx by ANFIS-FFA, with an example calculation.

mf_j	Consequent Parameters					Output Consequents	Weighted Output
	a_i	b_i	c_i	d_i	r_i		
mf_1	0.48	65.56	472.90	124.99	-329.20	0.48*53.3+65.56*2.09+472.90*0.79+124.99*0.11-329.20=221.09	9.15E-02
mf_2	5.51	-102.50	-478.90	306.31	463.30	197.59	1.79E-46
mf_3	6.62	100.83	1759.70	2997.03	495.60	2778.95	0.00E+00
mf_4	6.50	18.00	-286.20	2953.30	433.70	916.50	0.00E+00
mf_5	-6.63	62.90	-1686.40	2799.40	-246.92	-1491.56	-7.59E-87
mf_6	-6.63	-7.02	53.97	10.67	7.94	1276.14	0.00E+00
mf_7	0.38	-7.02	53.97	-10.67	7.94	54.61	5.46E+01
mf_8	2.98	-58.63	-1125.40	-2997.00	-495.60	-1677.51	0.00E+00
						Predicted Kx, Sum=54.68	

C. EXPLICIT CALCULATION PROCEDURE OF K_X BY ANFIS-FFA OPTIMIZED PARAMETERS

As mentioned previously, the ANFIS model is a black box system that has not provided the algebraic form explicitly. Another novel contribution of this research is hybridizing the FFA procedure with ANFIS model in the explicit calculation of Kx, using an extended database. The ANFIS models can be used as a trained program with its optimized inherent parameter values. ANFIS usually is used in a subprogram that receives input vector and produces corresponding output rather than the algebraic form. However, the algebraic form of the best model (M1) in matrix format is provided. The algebraic form of ANFIS-FFA for Kx estimations based on the eq. 14 is derived:

$$K_x = \sum_{j=1}^{nmf=8} w_j^n f_j = \sum_{j=1}^{nmf=8} \left[w_j^n \left(B \times a_j + H \times b_j + U \times c_j + U. \times d_j + r_j \right) \right] \quad (22)$$

where a_j, b_j, c_j, d_j and r_j are the optimized consequent parameters that are given in Table 9. w_j^n is the normalized matrix of weights derived by the membership degree from Gaussian function parameters and provided in Table 10.

The normalized weights are calculated using equations 9-12, and they are used in equation 22 to calculate the K_x value.

The main focus of the current study is providing an explicit calculation procedure for Kx based on the optimized ANFIS that has not yet reported in the previous studies clearly. An example of calculation procedure is provided in Tables 9 and 10. In this example H=2.09m; B=53.3m; U=0.79m/s; U∗ = 0.11m/s. The calculation steps for calculating the output of optimized ANFIS model for these values are as follows:

1- Use parameters of membership functions: The columns 2-9 in Table 9 give the s and c parameters of each membership function for each input parameter that are optimized and determined by FFA.
2- Calculate the output of membership functions: by using the optimized values of c and s in equation 10, the output of each membership function for every input parameter calculates, as the example calculations are provided bellow the Table 9. The output of each membership function in each parameter of B=53.3m; H=2.09 m; U=0.79 m/s; U∗ =0.11 m/s is calculated in columns 10-13 in Table 9.
3- Calculate the product of membership function outputs by using Eq.11: by multiplying the output of each membership function the product value is calculated in column 14 in Table 9.
4- Calculate the relative weight of each membership function by using Eq.12: this is calculated by dividing each row in column 14 to the total sum of column 14 and the results are given in column 15 in Table 9.
5- Use the optimized consequent parameters of each membership function. These FFA based optimized values are provided in column 2-6 in Table 10.
6- Calculate the consequent outputs, the second part that are in parentheses in Eq.13; these values are calculated in column 7 in Table 10.

TABLE 11. The raw data set used in ANFIS-FFA model development.

row	W(m)	H(m)	U(m/s)	U*(m/s)	Kx(m2/s)	row	W(m)	H(m)	U(m/s)	U*(m/s)	Kx(m2/s)	row	W(m)	H(m)	U(m/s)	U*(m/s)	Kx(m2/s)
1	53.3	2.09	0.79	0.11	46.45	31	49.2	1.11	0.94	0.08	331.1	61	24	1.56	0.71	0.04	9.6
2	28.96	0.3	0.35	0.04	53.73	32	0.4	0.11	0.46	0.06	0.01	62	0.2	0.06	0.51	0.03	0.04
3	0.4	0.1	0.55	0.07	0.03	33	116.4	3.66	0.45	0.06	227.6	63	17.1	0.39	0.16	0.12	9.1
4	158	4.3	0.19	0.01	41.1	34	0.2	0.11	0.83	0.05	0.06	64	37.99	0.95	0.25	0.06	9.1
5	0.2	0.09	0.58	0.03	0.05	35	0.6	0.12	0.31	0.05	0.67	65	47.24	0.84	0.23	0.07	13.94
6	0.4	0.09	0.33	0.04	0.01	36	20.1	0.99	0.59	0.1	34.5	66	0.4	0.11	0.62	0.07	0.05
7	23.77	1.6	0.67	0.04	5.96	37	56.3	0.67	0.18	0.05	19.7	67	24.9	1.1	0.32	0.05	6.5
8	24.18	1.56	0.71	0.04	17.7	38	535.7	9.07	1.47	0.1	1418	68	26.82	1.68	0.06	0	0.17
9	36.6	0.81	0.29	0.07	23.23	39	173	1.4	0.52	0.04	85.39	69	35	2.5	0.04	0	0.2
10	31.55	1.37	0.07	0.01	0.44	40	46.9	0.86	0.28	0.07	13.93	70	50.6	1.25	0.62	0.06	81.47
11	533.4	4.9	1.05	0.07	457.7	41	19.51	1.2	0.45	0.1	32.51	71	0.2	0.14	0.52	0.03	0.03
12	21	1.4	0.28	0.01	7.2	42	103.6	2.04	0.56	0.05	315.9	72	0.2	0.09	0.47	0.02	0.03
13	18.2	0.84	0.6	0.1	46.45	43	12.5	0.36	0.31	0.04	6.87	73	19.53	0.24	0.1	0.03	110.8
14	23.47	0.7	0.52	0.1	101.5	44	53.4	3.74	0.39	0.06	20	74	32.31	0.79	0.42	0.07	26.17
15	37.34	0.38	0.22	0.05	32	45	30.78	0.57	0.29	0.11	81.79	75	97.54	1.15	0.32	0.06	119.8
16	0.4	0.09	0.35	0.04	0.01	46	25.36	1.58	0.11	0.01	1.86	76	0.4	0.15	0.63	0.08	0.03
17	34.14	2.47	0.82	0.18	65.03	47	0.4	0.14	0.52	0.06	0.04	77	111	7.1	0.37	0.05	5.4
18	161.5	4	0.29	0.06	130.5	48	83	0.61	0.16	0.05	6.01	78	24.4	1.56	0.67	0.04	9.57
19	64.01	0.76	0.67	0.27	34.84	49	49	8.07	0.27	0.02	3	79	100	4.4	0.03	0	0.2
20	30.63	2.03	0.6	0.08	21.5	50	0.2	0.07	0.75	0.04	0.08	80	32	0.5	0.24	0.04	52.2
21	0.2	0.07	0.75	0.04	0.05	51	33.8	0.85	0.15	0.05	26.8	81	30.48	0.59	0.29	0.11	113.4
22	10.97	0.52	0.21	0.07	17.5	52	35.05	0.32	0.21	0.04	6.5	82	107	5.1	0.16	0.03	0.15
23	48.46	0.88	0.34	0.08	205.8	53	39.78	1.52	0.27	0.02	30.31	83	47.24	0.85	0.24	0.07	13.94
24	0.4	0.11	0.39	0.05	0.02	54	15.9	0.2	0.39	0.05	7.1	84	0.2	0.06	0.51	0.03	0.05
25	43.28	0.56	0.29	0.07	120.2	55	0.2	0.09	0.58	0.03	0.06	85	867	16.76	1.27	0.06	295.1
26	106.1	6.1	0.79	0.09	181	56	15.85	0.39	0.32	0.06	9.29	86	14.5	0.3	0.25	0.06	1.9
27	48.8	7.46	0.27	0.02	3	57	21.3	0.5	0.54	0.03	501.4	87	8.6	0.3	0.37	0.07	1.24
28	71.63	3.84	0.76	0.13	260.1	58	47.2	1.04	0.31	0.07	9.1	88	27.43	1.37	0.06	0.01	0.06
29	160.3	2.3	1.06	0.05	308.9	59	67.96	2.77	0.23	0.03	20.62	89	10	0.35	0.53	0.17	12.4
30	34.9	0.29	0.1	0.04	42	60	0.4	0.07	0.5	0.03	0.01	90	268.2	1.01	0.61	0.04	315.6

TABLE 11. ***(Continued.)*** **The raw data set used in ANFIS-FFA model development.**

row	W(m)	H(m)	U(m/s)	U*(m/s)	Kx(m2/s)	row	W(m)	H(m)	U(m/s)	U*(m/s)	Kx(m2/s)	row	W(m)	H(m)	U(m/s)	U*(m/s)	Kx(m2/s)
91	30.66	0.55	0.41	0.03	17.41	121	0.4	0.1	0.33	0.03	0	151	35	1.77	0.04	0.02	0.44
92	0.2	0.09	0.47	0.02	0.06	122	30.36	2.53	0.1	0.01	0.07	152	67.06	0.55	0.35	0.04	30.19
93	0.4	0.12	0.57	0.07	0.03	123	27.74	1.98	0.04	0	0.15	153	253.6	0.81	0.48	0.07	45.1
94	20	1.92	0.62	0.12	11.5	124	12.5	0.25	0.31	0.04	6.97	154	0.4	0.1	0.42	0.03	0.02
95	0.2	0.07	0.75	0.04	0.09	125	152.4	3.66	0.45	0.03	140	155	0.4	0.1	0.6	0.07	0.04
96	16.27	0.85	0.62	0.1	41.8	126	48.8	8.07	0.27	0.02	3	156	867	16.76	1.42	0.06	447.6
97	91.9	2.4	0.52	0.09	166.9	127	0.4	0.08	0.48	0.06	0.06	157	0.2	0.12	0.63	0.04	0.08
98	2.42	0.17	0.42	0.02	0.07	128	0.2	0.09	0.86	0.04	0.06	158	9.94	0.48	0.32	0.12	11
99	47.55	0.88	0.44	0.07	37.16	129	24.99	1.54	0.66	0.04	5.92	159	253.6	1.6	0.61	0.03	143.8
100	92.96	0.71	0.16	0.05	41.4	130	68.6	2.2	1.55	0.17	162.6	160	34.1	2.5	0.82	0.18	65
101	259	3.4	0.17	0.02	51.7	131	28.44	0.85	0.16	0.05	26.8	161	53.2	2.4	0.66	0.11	36.9
102	85	2.6	0.69	0.06	52	132	65.53	1.13	0.39	0.08	32.51	162	15.8	0.41	0.37	0.06	13.84
103	21.06	0.61	0.13	0.06	104.1	133	25	1.57	0.83	0.1	18	163	184	3.05	1.71	0.08	1490
104	0.4	0.07	0.68	0.04	0.13	134	59.44	0.76	0.68	0.07	53.3	164	11.4	0.75	0.41	0.06	8
105	0.9	0.45	0.7	0.03	0.08	135	0.6	0.13	0.77	0.11	1.26	165	248.1	4.82	0.31	0.07	143.8
106	25.9	0.9	0.34	0.07	32.5	136	30.36	3.53	0.05	0	0.09	166	0.4	0.09	0.34	0.04	0.01
107	19	0.4	0.16	0.12	9.9	137	12.2	0.5	0.23	0.03	14.7	167	13	0.6	0.48	0.24	6.8
108	182.9	3.29	1.55	0.08	1486	138	0.2	0.07	0.75	0.04	0.05	168	59.4	1.1	0.88	0.12	41.8
109	19.8	0.41	0.29	0.04	13.94	139	0.2	0.09	0.58	0.03	0.04	169	39.96	2.82	0.63	0.05	11.48
110	120	2	0.64	0.05	67	140	53.3	2.09	0.83	0.11	11.2	170	0.2	0.07	0.75	0.04	0.04
111	25.9	0.84	0.34	0.07	38.62	141	232	3.4	0.24	0.04	223.8	171	70.1	2.33	0.43	0.1	111.5
112	0.2	0.09	0.58	0.03	0.06	142	116.4	1.7	0.58	0.05	131.3	172	2.42	0.15	0.63	0.07	0.12
113	57.9	2.5	0.75	0.1	40.5	143	0.2	0.12	0.5	0.03	0.02	173	34.08	2.62	0.11	0.01	0.07
114	11.89	0.66	0.43	0.09	20.9	144	0.4	0.12	0.57	0.07	0.02	174	46.9	0.86	0.28	0.07	12.93
115	37.49	2.07	0.1	0.04	54.7	145	46.02	0.53	0.41	0.04	501.4	175	127.4	4.85	0.64	0.08	288.5
116	19.5	1.2	0.45	0.09	32.52	146	1.1	0.13	0.36	0.02	0.02	176	7.62	0.21	0.12	0.04	24.38
117	53.3	2.19	0.79	0.11	145.5	147	36.6	0.91	0.4	0.07	40.2	177	0.2	0.07	0.44	0.02	0.03
118	67.1	0.55	0.35	0.04	30.19	148	15.9	0.49	0.21	0.08	19.52	178	24.7	1.6	0.66	0.04	5.9
119	0.2	0.07	0.75	0.04	0.09	149	12.34	0.25	0.41	0.03	12.48	179	0.4	0.1	0.6	0.07	0.06
120	35.1	0.98	0.21	0.04	39.48	150	50.9	0.42	0.46	0.05	20.9	180	35	1.77	0.04	0.02	0.33

TABLE 11. ***(Continued.)*** **The raw data set used in ANFIS-FFA model development.**

row	W(m)	H(m)	U(m/s)	U*(m/s)	Kx(m2/s)	row	W(m)	H(m)	U(m/s)	U*(m/s)	Kx(m2/s)	row	W(m)	H(m)	U(m/s)	U*(m/s)	Kx(m2/s)
181	0.2	0.09	0.86	0.04	0.06	211	12.8	0.3	0.42	0.06	17.5	241	29.9	0.4	0.34	0.02	44
182	300	0.4	0.97	0.03	183.4	212	35.05	0.98	0.21	0.04	39.48	242	0.4	0.12	0.54	0.06	0.05
183	0.2	0.06	0.51	0.03	0.04	213	201.2	3.56	1.27	0.08	836.1	243	53.34	2.09	0.46	0.11	46.45
184	17.5	0.5	0.32	0.02	5.8	214	36.6	0.49	0.32	0.05	13.94	244	0.2	0.12	0.63	0.04	0.07
185	27.57	2.04	0.21	0.03	0.24	215	31.39	1.43	0.13	0.04	24.2	245	1.5	0.14	0.33	0.1	1.9
186	85.95	2.93	1.2	0.53	153.3	216	40.53	0.41	0.43	0.05	11.53	246	0.2	0.13	0.5	0.03	0.03
187	40.54	0.41	0.23	0.04	66.5	217	59.7	0.42	0.15	0.08	2.41	247	18.29	1.22	0.11	0.01	1.31
188	0.6	0.13	0.31	0.06	0.15	218	537.4	8.9	1.51	0.1	341.1	248	30.18	2.1	0.59	0.07	12
189	1.1	0.09	0.21	0.03	0.05	219	26.52	1.83	0.03	0	0.06	249	0.2	0.09	0.86	0.04	0.07
190	34.08	0.53	0.38	0.04	162.9	220	15.85	0.41	0.37	0.06	13.94	250	64	0.8	0.67	0.27	34.8
191	0.4	0.05	0.41	0.02	0.02	221	127	8.3	1.07	0.05	15.7	251	24.08	0.98	0.59	0.1	101.5
192	103.4	1.9	0.61	0.04	57.65	222	16	0.49	0.26	0.08	15.5	252	31.11	1.8	0.02	0	0.06
193	0.2	0.14	0.52	0.03	0.02	223	6.1	0.49	0.25	0.06	69	253	21.3	0.9	0.36	0.04	24.2
194	59.4	2.43	0.86	0.1	203.9	224	20.4	0.61	0.52	0.08	24.55	254	75	1.6	0.22	0.99	11.8
195	19.4	1.1	0.05	0.05	9.3	225	28.7	0.6	0.35	0.07	10.7	255	0.4	0.13	0.54	0.06	0.01
196	259	3.3	0.17	0.02	50.9	226	537.4	8.9	1.51	0.1	374.1	256	65.5	1.13	0.39	0.08	32.52
197	9.36	0.61	0.39	0.13	10.35	227	11	0.29	0.35	0.06	2.7	257	0.2	0.09	0.86	0.04	0.04
198	0.4	0.08	0.44	0.06	0.04	228	35.2	0.31	0.17	0.04	4.29	258	36	0.58	0.21	0.05	8.1
199	0.4	0.12	0.54	0.06	0.02	229	0.2	0.12	0.63	0.04	0.07	259	34.14	2.46	0.82	0.18	65.03
200	187	6.3	0.37	0.03	12.2	230	0.2	0.09	0.58	0.03	0.04	260	152.4	3.7	0.45	0.06	227.6
201	1.1	0.07	0.27	0.01	0.01	231	19.81	0.58	0.24	0.02	6.5	261	161.5	3.96	0.29	0.02	13
202	42.98	1.28	0.26	0.07	45.1	232	34.08	2.62	0.08	0	0.14	262	42.37	0.8	0.42	0.07	30.19
203	76	1.2	1.41	0.06	115.7	233	19.8	0.42	0.43	0.07	14.15	263	11.28	0.29	0.34	0.06	2.82
204	36	0.58	0.3	0.05	8.08	234	0.4	0.14	0.73	0.08	0.03	264	30	1.1	0.38	0.03	8
205	12	0.3	0.33	0.05	1.32	235	50.29	1.37	0.67	0.07	80.34	265	36.8	0.9	0.13	0.05	15.5
206	0.2	0.06	0.51	0.03	0.03	236	102	4.4	0.17	0.01	50.5	266	0.4	0.05	0.96	0.04	0.06
207	500.8	5.14	1.02	0.08	922.1	237	5	0.28	0.26	0.21	7.2	267	155.1	1.7	0.47	0.04	177.7
208	0.4	0.06	0.64	0.03	0.03	238	0.2	0.09	0.58	0.03	0.05	268	20.92	0.89	0.4	0.08	57.56
209	37.19	0.91	0.42	0.03	24.3	239	35.66	0.32	0.1	0.04	350	269	12.95	0.3	0.16	0.1	12.75
210	0.4	0.11	0.62	0.07	0.06	240	20	0.4	0.19	0.18	6.5	270	36.1	0.34	0.21	0.04	4.65

TABLE 11. ***(Continued.)*** **The raw data set used in ANFIS-FFA model development.**

row	W(m)	H(m)	U(m/s)	U*(m/s)	Kx(m2/s)	row	W(m)	H(m)	U(m/s)	U*(m/s)	Kx(m2/s)	row	W(m)	H(m)	U(m/s)	U*(m/s)	Kx(m2/s)
271	52.66	1.47	0.66	0.08	11.1	301	60	0.95	0.46	0.09	47	331	25.9	0.94	0.34	0.07	27.6
272	17.34	2.19	0.03	0	0.28	302	16.2	0.49	0.25	0.08	9.5	332	0.4	0.12	0.69	0.08	0.05
273	0.2	0.12	0.5	0.03	0.11	303	0.4	0.12	0.54	0.06	0.04	333	9	0.3	0.37	0.15	8.4
274	33.53	0.58	0.16	0.04	66.5	304	31.11	1.8	0.02	0	0.06	334	59.4	2.13	0.94	0.1	11.1
275	59	0.72	0.37	0.07	32	305	29.87	2.39	0.55	0.07	14.14	335	24.4	1.56	0.71	0.04	17.7
276	229	3.4	1.24	0.08	123	306	0.2	0.14	0.52	0.03	0.03	336	711.2	19.9	0.56	0.04	237.2
277	30.6	0.4	0.45	0.05	17.43	307	12.2	2.32	1.06	0.05	308.9	337	0.4	0.1	0.55	0.07	0.05
278	1.4	0.19	0.38	0.11	9.6	308	46.63	0.67	0.54	0.04	194	338	19.6	0.8	0.49	0.1	20.8
279	36.12	0.35	0.15	0.05	166	309	9.9	0.83	0.46	0.09	5.5	339	21.3	0.5	0.13	0.04	12.8
280	0.2	0.14	0.52	0.03	0.07	310	79.4	2.34	0.78	0.08	99.89	340	43.28	0.69	0.22	0.06	40.8
281	14.9	0.6	0.27	0.08	10.3	311	12.9	0.76	0.43	0.09	193.9	341	59.4	2.13	0.86	0.1	53.88
282	41.33	2.93	0.58	0.06	18.13	312	25.91	0.94	0.34	0.07	32.52	342	30.6	0.81	0.4	0.07	29.97
283	0.2	0.09	0.46	0.03	0.02	313	31.49	0.79	0.46	0.03	100.2	343	54.6	2.49	0.52	0.05	12.76
284	85.95	2.82	1.25	0.52	1799	314	0.4	0.13	0.44	0.06	0.02	344	7.6	3.45	0.68	0.05	0.5
285	1.1	0.18	0.22	0.03	0.07	315	211.5	2.19	0.41	0.03	169.5	345	10.8	0.4	0.32	0.06	8.29
286	153.6	2.27	1	0.06	98.22	316	97.5	1.1	0.32	0.06	33.8	346	25	0.56	1.01	0.14	13.94
287	13.41	0.81	0.37	0.08	13.94	317	127.4	4.75	0.64	0.08	668.9	347	37.8	1.89	0.21	0.02	0.19
288	13.7	0.9	1.29	0.55	2.9	318	15.8	0.5	0.27	0.08	15.1	348	0.4	0.14	0.73	0.08	0.06
289	0.2	0.12	0.5	0.03	0.05	319	47.5	0.87	0.44	0.07	37.16	349	202.7	1.35	0.39	0.07	92.9
290	103.6	2.04	0.58	0.05	315.9	320	59.44	1.1	0.88	0.12	41.81	350	31.13	2.1	0.03	0.01	0.17
291	183	5.7	0.11	0.02	10.9	321	0.2	0.09	0.86	0.04	0.06	351	176	3.4	1.61	0.08	64.9
292	196.6	3.11	1.53	0.08	891.9	322	0.4	0.12	0.58	0.07	0.02	352	0.6	0.13	0.31	0.03	0.05
293	48.7	0.55	0.26	0.05	37.8	323	17.37	1.23	0.04	0.05	14.7	353	253.6	1.62	0.61	0.04	194.1
294	15.36	1.71	0.06	0.01	0.1	324	18.29	0.63	0.33	0.05	16.66	354	63.7	0.46	0.1	0.06	29.3
295	13.4	0.81	0.37	0.08	13.94	325	43	1.23	0.63	0.08	59.3	355	21.03	0.48	0.52	0.07	25.9
296	16.8	0.5	0.24	0.08	24.6	326	0.6	0.13	0.53	0.08	0.63	356	45.11	2.26	0.04	0.01	0.1
297	0.4	0.03	0.68	0.03	0.07	327	40.2	0.7	0.23	0.06	8.8	357	36.58	0.91	0.4	0.07	39.48
298	33.53	0.78	0.19	0.05	10.7	328	0.4	0.09	0.46	0.07	0.05	358	49.99	0.95	0.32	0.07	29.6
299	0.2	0.06	0.51	0.03	0.04	329	40.54	0.4	0.19	0.06	100.3	359	0.2	0.12	0.63	0.04	0.05
300	194	6.3	0.22	0.04	474.6	330	16.7	0.5	0.2	0.08	16.8	360	13.4	0.91	0.37	0.08	13.94

TABLE 11. ***(Continued.)*** **The raw data set used in ANFIS-FFA model development.**

row	W(m)	H(m)	U(m/s)	U*(m/s)	Kx(m2/s)	row	W(m)	H(m)	U(m/s)	U*(m/s)	Kx(m2/s)	row	W(m)	H(m)	U(m/s)	U*(m/s)	Kx(m2/s)
361	34.45	2.19	0.07	0.02	0.21	391	37.06	0.77	0.41	0.07	234.7	421	24.99	0.45	0.41	0.08	25.9
362	158.2	2.3	1.04	0.06	217.9	392	10	0.63	0.55	0.3	13.5	422	120	7	0.91	0.04	33.9
363	53.34	2.1	0.46	0.11	46.45	393	27	1.1	0.44	0.01	10.3	423	67.1	0.98	0.88	0.11	41.81
364	50.9	0.52	0.46	0.05	20.9	394	167	0.2	0.47	0.16	24.4	424	0.2	0.09	0.86	0.04	0.1
365	25	1.21	0.73	0.08	27	395	37.8	1.89	0.05	0.01	0.19	425	51.2	0.65	0.66	0.04	79.6
366	9.14	0.41	0.27	0.09	243	396	20.42	0.52	0.24	0.02	6.77	426	71.63	3.84	0.77	0.13	260.1
367	21.49	2.87	0.02	0	0.02	397	85.3	2.4	1.74	0.15	464.6	427	29.26	0.73	0.31	0.02	12.73
368	0.2	0.12	0.63	0.04	0.05	398	24.99	0.58	1.01	0.14	13.94	428	701	17.51	0.56	0.04	43.14
369	18.29	0.41	0.22	0.04	8.85	399	18.3	0.4	0.15	0.12	20.7	429	14.02	0.24	0.32	0.03	20.13
370	46.18	0.67	0.38	0.08	88.13	400	867	16.76	1.34	0.06	139.7	430	28.65	0.58	0.54	0.04	36.89
371	54.89	1.84	0.84	0.09	11	401	18.6	0.39	0.14	0.12	9.85	431	48.34	2.61	0.56	0.05	11.5
372	51.21	0.65	0.62	0.04	29.6	402	230	3.5	1.08	0.09	155.9	432	0.2	0.09	0.86	0.04	0.07
373	0.4	0.09	0.32	0.04	0.02	403	34	2.5	0.13	0.01	1.7	433	0.2	0.07	0.75	0.04	0.08
374	36.58	0.92	0.4	0.07	39.48	404	49.68	0.41	0.15	0.08	29.3	434	202	4.6	0.18	0.04	71.7
375	160.3	1.74	0.47	0.04	177.7	405	45.11	2.26	0.05	0.01	0.27	435	21.77	1.58	0.31	0.06	6.5
376	99.97	2.5	0.3	0.11	166.9	406	59.44	2.13	0.67	0.11	55.74	436	867	16.76	1.49	0.06	471.7
377	55.78	2.26	0.69	0.1	36.93	407	10.8	0.41	0.29	0.04	10.94	437	0.2	0.09	0.47	0.02	0.02
378	0.4	0.1	0.6	0.07	0.04	408	71.6	3.8	0.76	0.13	260.1	438	48.5	1.2	0.21	0.07	14.8
379	34	0.85	0.15	0.06	9.5	409	0.6	0.13	0.53	0.12	1.08	439	32.6	0.3	0.43	0.05	9.29
380	10.53	0.29	0.35	0.06	3.36	410	75.6	2	0.74	0.14	88.9	440	0.4	0.06	0.65	0.03	0.06
381	18	0.85	0.6	0.1	21	411	24.38	0.71	0.52	0.08	25.55	441	0.2	0.12	0.5	0.03	0.05
382	14.02	0.38	0.19	0.1	9.1	412	42.21	0.69	0.23	0.06	23.54	442	29.61	1.08	0.36	0.05	0.5
383	0.4	0.08	0.67	0.03	0.05	413	300	0.3	1	0.03	271.1	443	35.1	0.32	0.21	0.04	4.65
384	0.2	0.12	0.91	0.05	0.06	414	41.45	1.04	0.07	0.09	10.3	444	15.13	0.44	0.06	0.05	38
385	0.4	0.08	0.45	0.05	0.03	415	63	1	0.32	0.09	22	445	1.1	0.14	0.24	0.03	0.08
386	0.2	0.11	0.83	0.05	0.11	416	127.4	4.75	0.64	0.08	668.9	446	9.14	0.21	0.13	0.06	22.46
387	18.3	0.84	0.52	0.1	21.4	417	35	2.5	0.11	0.01	1.4	447	19.2	1.43	0.27	0.02	3.1
388	78	1.2	1.42	0.03	290.4	418	202.7	1.35	0.39	0.07	92.9	448	0.4	0.05	0.96	0.04	0.15
389	13.34	0.49	0.24	0.08	15	419	16.31	0.67	0.2	0.02	0.52	449	100.3	2.13	0.42	0.03	50.78
390	15.85	0.43	0.37	0.05	13.94	420	0.6	0.13	0.77	0.16	6.12	450	0.4	0.08	0.48	0.06	0.03

TABLE 11. ***(Continued.)*** **The raw data set used in ANFIS-FFA model development.**

row	W(m)	H(m)	U(m/s)	U*(m/s)	Kx(m2/s)	row	W(m)	H(m)	U(m/s)	U*(m/s)	Kx(m2/s)	row	W(m)	H(m)	U(m/s)	U*(m/s)	Kx(m2/s)
451	182.9	2.23	0.93	0.07	464.5	469	0.2	0.07	0.75	0.04	0.09	487	0.2	0.09	0.58	0.03	0.07
452	19.81	0.52	0.43	0.07	16.26	470	25.91	0.94	0.34	0.07	32.51	488	16	0.49	0.27	0.08	20
453	24.25	0.36	0.04	0.09	1040	471	31.7	0.76	0.36	0.05	44	489	0.4	0.12	0.64	0.08	0.07
454	21.95	1.46	0.08	0.01	0.14	472	180.6	3.3	1.62	0.08	1487	490	15.7	0.2	0.36	0.04	69
455	19.8	0.52	0.43	0.07	16.26	473	12.4	0.45	0.24	0.08	15.4	491	42.21	0.69	0.23	0.06	40.8
456	0.4	0.11	0.52	0.07	0.03	474	44.2	1.4	0.99	0.14	184.6	492	37.62	2.01	0.08	0.01	0.16
457	21.64	0.61	0.08	0.04	12.8	475	11.58	0.4	0.22	0.09	1.9	493	0.2	0.14	0.52	0.03	0.05
458	21.95	1.46	0.11	0.01	0.66	476	0.2	0.11	0.83	0.05	0.05	494	33.4	1.4	0.2	0.03	54.7
459	33.87	0.53	0.36	0.06	176.3	477	25	1.38	0.77	0.09	20.5	495	0.2	0.12	0.63	0.04	0.11
460	47.43	2.71	0.56	0.05	11	478	103.6	2.05	0.56	0.05	129.1	496	50.9	0.42	0.46	0.05	20.9
461	0.2	0.09	0.86	0.04	0.07	479	161.5	0.4	0.34	0.02	44	497	0.2	0.12	0.63	0.04	0.05
462	0.6	0.13	0.53	0.05	0.27	480	70.1	2.4	0.43	0.1	111.5	498	24.4	0.71	0.52	0.08	25.55
463	19.5	1.3	0.45	0.09	33.52	481	25	1.4	0.78	0.09	15.5	499	0.4	0.13	0.61	0.07	0.02
464	86	2.94	1.2	0.51	153.3	482	0.4	0.16	0.58	0.07	0.03	500	61.72	2.47	0.23	0.03	12.45
465	59.44	2.13	0.67	0.11	55.74	483	40.5	0.4	0.23	0.04	6.5	501	42.4	0.8	0.42	0.07	30.19
466	0.2	0.06	0.51	0.03	0.04	484	35.8	0.58	0.21	0.05	19.7	502	47.5	0.87	0.44	0.07	29.16
467	0.2	0.12	0.63	0.04	0.07	485	0.4	0.12	0.54	0.06	0.03	503	38.3	2.16	0.08	0.01	0.09
468	9.9	0.92	0.52	0.1	5.1	486	0.4	0.07	0.67	0.04	0.09						

7- Calculate the weighted output of consequences by Eq.13. The result of this step is given in column 8 in Table 10.
8- Calculate the final Kx value by using Eq.14: this is the final result of predicted Kx for given input values and is calculated and provide at the end of Table 10 (Kx=54.68).

these steps are used in an excel workbook and for all of the data are repeated to calculate the final values of model outputs and the procedure can be used in all of other cases as an explicit calculation procedure of ANFIS instead of previous black box approaches that limited the applicability of ANFIS models.

The newly developed equation (Eq.22) and its constants and parameters in Tables 9-10 is another novel contribution of ANFIS-FFA models in K_x estimations by providing explicit ANFIS based equation. Consequently, the newly developed equation can put its results into practical and numerical applications of pollutant transport over a wide range of hydraulic and hydrologic riverflows in the simulation of pollutant transport.

According to the statistical evaluations and one-by-one comparisons of ANFIS-FFA, ANFIS and existing equations, it is concluded that the ANFIS-FFA model shows a superior accuracy versus the others. The evaluation of the statistical indices of ANFIS-FFA and ANFIS demonstrates that hybrid training of the ANFIS with FFA is valuable because it provides a valuable improvement in the accuracy, generality and robustness of ANFIS to estimate the longitudinal dispersion in lack of the concentration profile measures.

IV. CONCLUSION

In this paper, the ANFIS model trained with FFA is implemented to estimate the K_x for pollutant transport. A global and general database of K_x contains 503 data records, is collected and assessed by the SSMD technique for subset selection. The sensitivity results attained in ANFIS-FFA with different input combinations of dominant variables showed that using the U, U*, B and H variables led to the best results. Evaluation of ANFIS-FFA and existing equations suggests that the developed hybridization scheme outperforms the existing approaches in dimensional and Non-dimensional format of the results. The newly developed methodology estimated about 96% of K_x values with <5% error as presented by ellipse bounds. In conclusion, the ANFIS-FFA proved to be a consistent tool for pollutant dispersion estimations under a wide range of flow conditions, especially from small to large rivers. When the complexity of pollutant dispersion increases and generality of existing equations are wasted, due to a lack of their calibration data and inherent weaknesses of them, the newly developed model has valuable practical strength. The new developed explicit matrix formula (Eq.22) is a novel mathematical derivation of ANFIS-FFA model results. It can be used in hybridizing with numerical models of pollutant transport and this is one of the main contributions of the present paper in extending the applicability of black-box models of ANFIS-FFA in an explicit formulae. The proposed approach for the derivation of explicit equations based on ANFIS-FFA can be used in further studies of future ANFIS models.

APPENDIX

See Table 11.

REFERENCES

[1] P. Burns and E. Meiburg, "Sediment-laden fresh water above salt water: Linear stability analysis," *J. Fluid Mech.*, vol. 691, pp. 279–314, Jan. 2012, doi: 10.1017/jfm.2011.474.
[2] M. Cassol, S. Wortmann, and U. Rizza, "Analytic modeling of two-dimensional transient atmospheric pollutant dispersion by double GITT and laplace transform techniques," *Environ. Model. Softw.*, vol. 24, no. 1, pp. 144–151, Jan. 2009, doi: 10.1016/j.envsoft.2008.06.001.
[3] G. Jin, H. Tang, L. Li, and D. A. Barry, "Prolonged river water pollution due to variable-density flow and solute transport in the riverbed," *Water Resour. Res.*, vol. 51, no. 4, pp. 1898–1915, Apr. 2015.
[4] I. M. H. R. Antunes, M. T. D. Albuquerque, S. F. Oliveira, and G. Sánz, "Predictive scenarios for surface water quality simulation–A watershed case study," *Catena*, vol. 170, pp. 283–289, Nov. 2018.
[5] A. Fick, "On liquid diffusion," *Phil. Mag. Ser.*, vol. 4, vol. 10, no. 63, pp. 30–39.
[6] Y. Wang and W. Huai, "Estimating the longitudinal dispersion coefficient in straight natural rivers," *J. Hydraulic Eng.*, vol. 142, no. 11, Nov. 2016, Art. no. 04016048.
[7] Y.-F. Wang, W.-X. Huai, and W.-J. Wang, "Physically sound formula for longitudinal dispersion coefficients of natural rivers," *J. Hydrol.*, vol. 544, pp. 511–523, Jan. 2017.
[8] V. Ramšak, V. Malačič, M. Ličer, J. Kotnik, M. Horvat, and D. Žagar, "High-resolution pollutant dispersion modelling in contaminated coastal sites," *Environ. Res.*, vol. 125, pp. 103–112, Aug. 2013.
[9] M. Aghababaei, A. Etemad-Shahidi, E. Jabbari, and M. Taghipour, "Estimation of transverse mixing coefficient in straight and meandering streams," *Water Resour. Manage.*, vol. 31, no. 12, pp. 3809–3827, Sep. 2017, doi: 10.1007/s11269-017-1708-4.
[10] F. Sonnenwald, J. R. Hart, P. West, V. R. Stovin, and I. Guymer, "Transverse and longitudinal mixing in real emergent vegetation at low velocities," *Water Resour. Res.*, vol. 53, no. 1, pp. 961–978, Jan. 2017.
[11] I. W. Seo and T. S. Cheong, "Predicting longitudinal dispersion coefficient in natural streams," *J. Hydraulic Eng.*, vol. 124, no. 1, pp. 25–32, Jan. 1998.
[12] L. Zeng, Z. Wu, X. Fu, and G. Wang, "Performance of the analytical solutions for Taylor dispersion process in open channel flow," *J. Hydrol.*, vol. 528, pp. 301–311, Sep. 2015.
[13] G. I. Taylor, "Dispersion of soluble matter in solvent flowing slowly through a tube," *Proc. Roy. Soc. London, A, Math. Phys. Sci.*, vol. 219, no. 1137, pp. 186–203, 1953.
[14] G. I. Taylor, "The dispersion of matter in turbulent flow through a pipe," *Proc. Roy. Soc. London, A, Math. Phys. Sci.*, vol. 223, no. 1155, pp. 446–468, May 1954.
[15] H. Riahi-Madvar, S. A. Ayyoubzadeh, E. Khadangi, and M. M. Ebadzadeh, "An expert system for predicting longitudinal dispersion coefficient in natural streams by using ANFIS," *Expert Syst. Appl.*, vol. 36, no. 4, pp. 8589–8596, May 2009.
[16] H. B. Fischer, "The mechanics of dispersion in natural streams," *J. Hydraulics Division*, vol. 93, no. 6, pp. 187–216, 1967.
[17] G. Tayfur and V. P. Singh, "Predicting longitudinal dispersion coefficient in natural streams by artificial neural network," *J. Hydraulic Eng.*, vol. 131, no. 11, pp. 991–1000, Nov. 2005.
[18] B. Tutmez and M. Yuceer, "Regression kriging analysis for longitudinal dispersion coefficient," *Water Resour. Manage.*, vol. 27, no. 9, pp. 3307–3318, Jul. 2013.
[19] I. W. Seo and K. O. Baek, "Estimation of the longitudinal dispersion coefficient using the velocity profile in natural streams," *J. Hydraulic Eng.*, vol. 130, no. 3, pp. 227–236, Mar. 2004.
[20] R. Noori, Z. Deng, A. Kiaghadi, and F. T. Kachoosangi, "How reliable are ANN, ANFIS, and SVM techniques for predicting longitudinal dispersion coefficient in natural rivers?" *J. Hydraulic Eng.*, vol. 142, no. 1, 2015, Art. no. 04015039, doi: 10.1061/(ASCE)HY.1943-7900.0001062.

[21] W. Huai, H. Shi, S. Song, and S. Ni, "A simplified method for estimating the longitudinal dispersion coefficient in ecological channels with vegetation," *Ecol. Indicators*, vol. 92, pp. 91–98, Sep. 2018, doi: 10.1016/j.ecolind.2017.05.015.

[22] M. Farzadkhoo, A. Keshavarzi, H. Hamidifar, and M. Javan, "Sudden pollutant discharge in vegetated compound meandering rivers," *Catena*, vol. 182, Nov. 2019, Art. no. 104155.

[23] M. Najafzadeh and A. Tafarojnoruz, "Evaluation of neuro-fuzzy GMDH-based particle swarm optimization to predict longitudinal dispersion coefficient in rivers," *Environ. Earth Sci.*, vol. 75, no. 2, p. 157, Jan. 2016.

[24] J. W. Elder, "The dispersion of marked fluid in turbulent shear flow," *J. Fluid Mech.*, vol. 5, no. 4, pp. 544–560, May 1959.

[25] R. S. McQuivey and T. N. Keefer, "Simple method for predicting dispersion in streams," *J. Environ. Eng. Division*, vol. 100, no. 4, pp. 997–1011, 1974.

[26] H. B. Fischer, "Discussion of 'simple method for predicting dispersion in streams' by RS McQuivey and TN Keefer," *J. Environ. Eng.*, vol. 504, no. 101, p. 337, 1975.

[27] H. Liu, "Predicting dispersion coefficient of streams," *J. Environ. Eng. Division*, vol. 103, no. 1, pp. 59–69, 1977.

[28] Y. Iwasa, "Predicting longitudinal disperdsion coefficient in open-channel flows," in *Proc. Int. Symp. Environ. Hydraulics*, 1991, pp. 505–510.

[29] A. D. Koussis and J. Rodríguez-Mirasol, "Hydraulic estimation of dispersion coefficient for streams," *J. Hydraulic Eng.*, vol. 124, no. 3, pp. 317–320, Mar. 1998.

[30] Z.-Q. Deng, V. P. Singh, and L. Bengtsson, "Longitudinal dispersion coefficient in straight rivers," *J. Hydraulic Eng.*, vol. 127, no. 11, pp. 919–927, Nov. 2001.

[31] S. M. Kashefipour and R. A. Falconer, "Longitudinal dispersion coefficients in natural channels," *Water Res.*, vol. 36, no. 6, pp. 1596–1608, Mar. 2002.

[32] I. Papadimitrakis and I. Orphanos, "Longitudinal dispersion characteristics of rivers and natural streams in greece," *Water, Air, Soil Pollut., Focus*, vol. 4, no. 4/5, pp. 289–305, Oct. 2004.

[33] Z. Ahmad, "Mixing length for establishment of longitudinal dispersion in streams," *Int. J. Model. Simul.*, vol. 29, no. 2, pp. 127–136, Jan. 2009, doi: 10.1080/02286203.2009.11442518.

[34] Z. Fuat Toprak and M. E. Savci, "Longitudinal dispersion coefficient modeling in natural channels using fuzzy logic," *CLEAN-Soil, Air, Water*, vol. 35, no. 6, pp. 626–637, Dec. 2007.

[35] Z. F. Toprak and H. K. Cigizoglu, "Predicting longitudinal dispersion coefficient in natural streams by artificial intelligence methods," *Hydrol. Processes*, vol. 22, no. 20, pp. 4106–4129, Sep. 2008.

[36] R. Noori, A. Karbassi, A. Farokhnia, and M. Dehghani, "Predicting the longitudinal dispersion coefficient using support vector machine and adaptive neuro-fuzzy inference system techniques," *Environ. Eng. Sci.*, vol. 26, no. 10, pp. 1503–1510, Oct. 2009.

[37] H. M. Azamathulla and A. A. Ghani, "Genetic programming for predicting longitudinal dispersion coefficients in streams," *Water Resour. Manage.*, vol. 25, no. 6, pp. 1537–1544, Apr. 2011, doi: 10.1007/s11269-010-9759-9.

[38] A. M. A. Sattar and B. Gharabaghi, "Gene expression models for prediction of longitudinal dispersion coefficient in streams," *J. Hydrol.*, vol. 524, pp. 587–596, May 2015.

[39] H. Riahi-Madvar, M. Dehghani, A. Seifi, and V. P. Singh, "Pareto optimal multigene genetic programming for prediction of longitudinal dispersion coefficient," *Water Resour. Manage.*, vol. 33, no. 3, pp. 905–921, Feb. 2019.

[40] H. M. Azamathulla and F.-C. Wu, "Support vector machine approach for longitudinal dispersion coefficients in natural streams," *Appl. Soft Comput.*, vol. 11, no. 2, pp. 2902–2905, Mar. 2011, doi: 10.1016/j.asoc.2010.11.026.

[41] M. J. Alizadeh, D. Ahmadyar, and A. Afghantoloee, "Improvement on the existing equations for predicting longitudinal dispersion coefficient," *Water Resour. Manage.*, vol. 31, no. 6, pp. 1777–1794, Apr. 2017, doi: 10.1007/s11269-017-1611-z.

[42] X. Li, H. Liu, and M. Yin, "Differential evolution for prediction of longitudinal dispersion coefficients in natural streams," *Water Resour. Manage.*, pp. 5245–5260, Oct. 2013.

[43] R. Noori, B. Ghiasi, H. Sheikhian, and J. F. Adamowski, "Estimation of the dispersion coefficient in natural rivers using a granular computing model," *J. Hydraulic Eng.*, vol. 143, no. 5, 2017, Art. no. 04017001, doi: 10.1061/(ASCE)HY.1943-7900.0001276.

[44] M. R. Balf, R. Noori, R. Berndtsson, A. Ghaemi, and B. Ghiasi, "Evolutionary polynomial regression approach to predict longitudinal dispersion coefficient in rivers," *J. Water Supply: Res. Technol.-Aqua*, vol. 67, no. 5, pp. 447–457, 2018, doi: 10.2166/aqua.2018.021.

[45] Z. M. Yaseen, I. Ebtehaj, H. Bonakdari, R. C. Deo, A. Danandeh Mehr, W. H. M. W. Mohtar, L. Diop, A. El-shafie, and V. P. Singh, "Novel approach for streamflow forecasting using a hybrid ANFIS-FFA model," *J. Hydrol.*, vol. 554, pp. 263–276, Nov. 2017.

[46] X.-S. Yang, "Firefly algorithms for multimodal optimization," in *Proc. Int. Symp. Stochastic Algorithms*. Berlin, Germany: Springer, Oct. 2009, pp. 169–178.

[47] S. Łukasik and S. Żak, "Firefly algorithm for continuous constrained optimization tasks," in *Proc. Int. Conf. Comput. Collective Intell.*, Oct. 2009, pp. 97–106.

[48] X. S. Yang, "Firefly algorithm, stochastic test functions and design optimisation," *Int. J. Bio-Inspired Comput.*, vol. 2, no. 2, pp. 78–84, 2010.

[49] A. Kavousi-Fard, H. Samet, and F. Marzbani, "A new hybrid modified firefly algorithm and support vector regression model for accurate short term load forecasting," *Expert Syst. Appl.*, vol. 41, no. 13, pp. 6047–6056, Oct. 2014.

[50] T. Xiong, Y. Bao, and Z. Hu, "Multiple-output support vector regression with a firefly algorithm for interval-valued stock price index forecasting," *Knowl.-Based Syst.*, vol. 55, pp. 87–100, Jan. 2014.

[51] H. Azimi, H. Bonakdari, I. Ebtehaj, and D. G. Michelson, "A combined adaptive neuro-fuzzy inference system–firefly algorithm model for predicting the roller length of a hydraulic jump on a rough channel bed," *Neural Comput. Appl.*, vol. 29, pp. 249–258, Aug. 2016, doi: 10.1007/s00521-016-2560-9.

[52] I. Ebtehaj and H. Bonakdari, "A support vector regression-firefly algorithm-based model for limiting velocity prediction in sewer pipes," *Water Sci. Technol.*, vol. 73, no. 9, pp. 2244–2250, May 2016.

[53] I. Ebtehaj, H. Bonakdari, S. Shamshirband, Z. Ismail, and R. Hashim, "New approach to estimate velocity at limit of deposition in storm sewers using vector machine coupled with firefly algorithm," *J. Pipeline Syst. Eng. Pract.*, vol. 8, no. 2, May 2017, Art. no. 04016018.

[54] M. A. Ghorbani, S. Shamshirband, D. Zare Haghi, A. Azani, H. Bonakdari, and I. Ebtehaj, "Application of firefly algorithm-based support vector machines for prediction of field capacity and permanent wilting point," *Soil Tillage Res.*, vol. 172, pp. 32–38, Sep. 2017.

[55] Q. Fu, R. Jiang, Z. Wang, and T. Li, "Optimization of soil water characteristic curves parameters by modified firefly algorithm," *Trans. Chin. Soc. Agricult. Eng.*, vol. 31, no. 11, pp. 117–122, 2015.

[56] E. Emary, H. M. Zawbaa, K. K. A. Ghany, A. E. Hassanien, and B. Parv, "Firefly optimization algorithm for feature selection," in *Proc. 7th Balkan Conf. Informat. Conf. (BCI)*, 2015, p. 26.

[57] H. B. Fischer and N. H. Brooks, "Longitudinal dispersion in laboratory and natural streams," California Inst. Technol., Pasadena, CA, USA, Tech. Rep. KH-R-12, 1996.

[58] K. R. Taylor, "Travel time and concentration attenuation of a soluble dye in the Monocacyriver, Maryland," Maryland Geol. Surv., Baltimore, MD, USA, Tech. Rep. 9, 1970.

[59] C. F. Nordin and G. V. Sabol, *Empirical Data on Longitudinal Dispersion in Rivers*. Reston,VA, USA: US Geological Survey, 1974.

[60] A. C. Miller and E. V. Richardson, "Diffusion and dispersion on convective model of longitudinal dispersion," *J. Hydraulics Division*, vol. 100, no. HY1, pp. 159–171, 1974.

[61] R. S. McQuivey and T. N. Keefer, "Dispersion-Mississipi river below Balton Rough 1," *J. Hydraulics Division*, vol. 102, no. 10, pp. 1423–1425, 1976.

[62] S. Beltaos, "An interpretation of longitudinal dispersion data in rivers," Transp. Surface Water Eng. Division, Alberta Res. Council, Edmonton, AB, Canada, Tech. Rep. SER 78-3, 1978.

[63] H. Hou and B. A. Christensen, "Influence of equivalent sand roughness on the dispersion coefficient in laboratory and natural stream," in *Proc. 3rd Annu. Symp. Waterways, Harbors Coastal. Eng. Diversions (ASCE)*, vol. 2. Fort Collins, CO, USA: Colorado State Univ., 1976, pp. 1179–1198.

[64] A. J. Calandro, "Time of travel of solute contaminants in streams," U.S. Geol. Surv., Water Resour., Reston, VA, USA, Tech. Rep. 17, 1978.

[65] T. J. Day, "Longitudinal dispersion in natural channels," *Water Resour. Res.*, vol. 1, pp. 909–918, 1975.

[66] R. W. James, Jr., and B. M. Helinsky, "Time of travel and dispersion in the Jones Falls, Baltimore, Maryland," U.S. Geol. Surv., Water Resour. Investigations, Reston, VA, USA, Tech. Rep. 8-4203, 1984.

[67] J. B. Graf, ''Travel time and longitudinal dispersion in Illinois streams,'' U.S. Geol. Surv., Reston, VA, USA, Tech. Rep. 84-468, 1984.
[68] U. P. Singh, ''Dispersion of conservative pollutant,'' Ph.D. dissertation, Univ. Roorkee, Roorkee, India, 1987.
[69] M. L. Carr and C. R. Rehmann, ''Measuring the dispersion coefficient with acoustic Doppler current profilers,'' *J. Hydraulic Eng.*, vol. 133, no. 8, pp. 977–982, 2007, doi: 10.1061/(ASCE)0733-9429(2007)133:8(977).
[70] O. Bozorg-Haddad, M. Zarezadeh-Mehrizi, M. Abdi-Dehkordi, H. A. Loáiciga, and M. A. Mariño, ''A self-tuning ANN model for simulation and forecasting of surface flows,'' *Water Resour. Manage.*, vol. 30, no. 9, pp. 2907–2929, Jul. 2016, doi: 10.1007/s11269-016-1301-2.
[71] K. Doycheva, G. Horn, C. Koch, A. Schumann, and M. König, ''Assessment and weighting of meteorological ensemble forecast members based on supervised machine learning with application to runoff simulations and flood warning,'' *Adv. Eng. Informat.*, vol. 33, pp. 427–439, Aug. 2017.
[72] M. Snarey, N. K. Terrett, P. Willett, and D. J. Wilton, ''Comparison of algorithms for dissimilarity-based compound selection,'' *J. Mol. Graph. Model.*, vol. 15, no. 6, pp. 372–385, Dec. 1997.
[73] R. W. Kennard and L. A. Stone, ''Computer aided design of experiments,'' *Technometrics*, vol. 11, no. 1, pp. 137–148, Feb. 1969.
[74] M. Lajiness and I. Watson, ''Dissimilarity-based approaches to compound acquisition,'' *Current Opinion Chem. Biol.*, vol. 12, no. 3, pp. 366–371, Jun. 2008.
[75] P. Camus, F. J. Mendez, R. Medina, and A. S. Cofiño, ''Analysis of clustering and selection algorithms for the study of multivariate wave climate,'' *Coastal Eng.*, vol. 58, no. 6, pp. 453–462, Jun. 2011, doi: 10.1016/j.coastaleng.2011.02.003.
[76] R. Memarzadeh, H. Ghayoumi Zadeh, M. Dehghani, H. Riahi-Madvar, A. Seifi, and S. M. Mortazavi, ''A novel equation for longitudinal dispersion coefficient prediction based on the hybrid of SSMD and whale optimization algorithm,'' *Sci. Total Environ.*, vol. 716, May 2020, Art. no. 137007, doi: 10.1016/j.scitotenv.2020.137007.
[77] L. A. Zadeh, ''Information and control,'' *Fuzzy sets*, vol. 8, no. 3, pp. 338–353, 1965.
[78] P. C. Nayak, K. P. Sudheer, and K. S. Ramasastri, ''Fuzzy computing based rainfall-runoff model for real time flood forecasting,'' *Hydrol. Processes*, vol. 19, no. 4, pp. 955–968, Mar. 2005.
[79] M. Firat and M. Güngör, ''Hydrological time-series modelling using an adaptive neuro-fuzzy inference system,'' *Hydrol. Processes*, vol. 22, no. 13, pp. 2122–2132, Jun. 2008.
[80] H. Riahi-Madvar and A. Seifi, ''Uncertainty analysis in bed load transport prediction of gravel bed rivers by ANN and ANFIS,'' *Arabian J. Geosci.*, vol. 11, no. 21, Nov. 2018, doi: 10.1007/s12517-018-3968-6.
[81] F.-J. Chang and Y.-T. Chang, ''Adaptive neuro-fuzzy inference system for prediction of water level in reservoir,'' *Adv. Water Resour.*, vol. 29, no. 1, pp. 1–10, Jan. 2006, doi: 10.1016/j.advwatres.2005.04.015.
[82] M. Dehghani, H. Riahi-Madvar, F. Hooshyaripor, A. Mosavi, S. Shamshirband, E. Zavadskas, and K.-W. Chau, ''Prediction of hydropower generation using grey wolf optimization adaptive neuro-fuzzy inference system,'' *Energies*, vol. 12, no. 2, p. 289, Jan. 2019, doi: 10.3390/en12020289.
[83] M. F. Allawi, O. Jaafar, F. Mohamad Hamzah, N. S. Mohd, R. C. Deo, and A. El-Shafie, ''Reservoir inflow forecasting with a modified coactive neuro-fuzzy inference system: A case study for a semi-arid region,'' *Theor. Appl. Climatol.*, vol. 134, nos. 1–2, pp. 545–563, Oct. 2018, doi: 10.1007/s00704-017-2292-5.
[84] A. Shabri, ''A hybrid wavelet analysis and adaptive neuro-fuzzy inference system for drought forecasting,'' *Appl. Math. Sci.*, vol. 8, pp. 6909–6918, 2014.
[85] B. Kurtulus and M. Razack, ''Modeling daily discharge responses of a large karstic aquifer using soft computing methods: Artificial neural network and neuro-fuzzy,'' *J. Hydrol.*, vol. 381, nos. 1–2, pp. 101–111, Feb. 2010.
[86] H. Tabari, O. Kisi, A. Ezani, and P. Hosseinzadeh Talaee, ''SVM, ANFIS, regression and climate based models for reference evapotranspiration modeling using limited climatic data in a semi-arid highland environment,'' *J. Hydrol.*, vols. 444–445, pp. 78–89, Jun. 2012.
[87] V. Nourani, H. Gökçekuş, and I. K. Umar, ''Artificial intelligence based ensemble model for prediction of vehicular traffic noise,'' *Environ. Res.*, vol. 180, Jan. 2020, Art. no. 108852.
[88] M. Mahmoodabadi and R. Rezaei Arshad, ''Long-term evaluation of water quality parameters of the Karoun River using a regression approach and the adaptive neuro-fuzzy inference system,'' *Mar. Pollut. Bull.*, vol. 126, pp. 372–380, Jan. 2018.
[89] H.-T. Ouyang, ''Input optimization of ANFIS typhoon inundation forecast models using a multi-objective genetic algorithm,'' *J. Hydro-Environ. Res.*, vol. 19, pp. 16–27, Mar. 2018.
[90] A. Sei and H. Riahi-Madvar, ''Estimating daily reference evapotranspiration using hybrid gamma test-least square support vector machine, gamma test-ANN, and gamma test-ANFIS models in an arid area of Iran,'' *J. Water Climate Change*, vol. 11, no. 1, pp. 217–240, 2020, doi: 10.2166/wcc.2018.003.
[91] C. W. Dawson, R. J. Abrahart, and L. M. See, ''HydroTest: A Web-based toolbox of evaluation metrics for the standardised assessment of hydrological forecasts,'' *Environ. Model. Softw.*, vol. 22, pp. 1034–1052, 2007, doi: 10.1016/j.envsoft.2006.06.008.
[92] M. Dehghani, B. Saghafian, F. Nasiri Saleh, A. Farokhnia, and R. Noori, ''Uncertainty analysis of streamflow drought forecast using artificial neural networks and monte-carlo simulation,'' *Int. J. Climatol.*, vol. 34, no. 4, pp. 1169–1180, Mar. 2014, doi: 10.1002/joc.3754.
[93] K. E. Taylor, ''Summarizing multiple aspects of model performance in a single diagram,'' *J. Geophys. Res., Atmos.*, vol. 106, no. D7, pp. 7183–7192, Apr. 2001.
[94] W. R. White, H. Milli, and A. D. Crabbe, ''Sediment transport: An appraisal methods,'' Perform. Theor. Methods Appl. Flume Field Data, Wallingford, U.K., Tech. Rep. 1T119, 1973.
[95] R. Noori, A. Khakpour, B. Omidvar, and A. Farokhnia, ''Comparison of ANN and principal component analysis-multivariate linear regression models for predicting the river flow based on developed discrepancy ratio statistic,'' *Expert Syst. Appl.*, vol. 37, no. 8, pp. 5856–5862, Aug. 2010.
[96] R. Noori, A. R. Karbassi, H. Mehdizadeh, M. Vesali-Naseh, and M. S. Sabahi, ''A framework development for predicting the longitudinal dispersion coefficient in natural streams using an artificial neural network,'' *Environ. Prog. Sustain. Energy*, vol. 30, no. 3, pp. 439–449, Oct. 2011.

HOSSIEN RIAHI-MADVAR received the Ph.D. degree in water structures engineering from the Tarbiat Modares University of Tehran, Iran. He is currently a Lecturer at the Vali-e-Asr University of Rafsanjani, Iran. He has published over 70 articles in peer reviewed journals/conferences. His current research interests are hydro-informatics, artificial intelligence applications in water engineering and uncertainty analysis, and the application of soft computing and image processing techniques for real world problems.

MAJID DEHGHANI received the B.Sc. and M.Sc. degrees in the field of hydrology and water resource management and the Ph.D. degree in water resources in 2014. He is currently an Assistant Professor at the Vali-e-Asr University of Rafsanjan. He have had published extensively in the field of hydrological modeling, during his Ph.D. degree. He has been coauthoring more than 60 textbooks, books, book chapters, and journal articles in the field of hydrology.

KULWINDER SINGH PARMAR received the Ph.D. degree in the area of mathematical modeling from the Non-Linear Dynamics Research Lab, Department of Mathematics, Guru Gobind Singh Indraprastha University, New Delhi. He is currently an Assistant Professor at the Department of Mathematics, I. K. Gujral Punjab Technical University, Jalandhar, India. He published more than 30 research articles in the area of mathematical modeling. Three Ph.D. research scholars are working currently with him.

NARJES NABIPOUR received the degree in computer science from expertise in machine learning modeling. She is currently a Researcher with Duy Tan University, Vietnam. She is also a Complex Systems Data Scientist with a focus on climate data. She has taught advanced statistics and data science for more than five years. She has coauthored in various journals. Her main research interests are prediction models, causal discovery, and causal inference based on graphical models and deep learning.

SHAHABODDIN SHAMSHIRBAND received the M.Sc. degree in artificial intelligence and the Ph.D. degree in computer science from the University of Malaya, Kuala Lumpur, Malaysia. He is currently an Adjunct Professor at Ton Duc Thang University, Vietnam, an Adjunct Faculty at Iran Science and Technology University, Iran, an Academic Faculty at IAUC, Iran, a Faculty Member at the University of Malaya, Malaysia, and a Postdoctoral Research Fellow. He has published more than 200 articles, 100 in refereed international SCI-IF journals, 25 international conference proceedings, and ten books with more than 7000 citations in Google Scholar (with h-index of 29), and ResearchGate RG Score of 47. His major academic interests are in computational intelligence and data mining in multidisciplinary fields. He has worked on various funded projects. He is on the editorial board of journals and has served as a guest editor for journals. His articles are ranked in the highly cited papers and most downloaded papers from the top 10 % (2013 till now) in computer science according to the WoS.